UV-Protective Compounds in Sea Ice-Associated Algae in the Canadian Arctic

by

Ashley Elliott

A Thesis submitted to the Faculty of Graduate Studies of

The University of Manitoba

In partial fulfilment of the requirement of the degree of

MASTER OF SCIENCE

Department of Environment and Geography

University of Manitoba

Winnipeg

Abstract

Marine phytoplankton are known to produce UV-absorbing compounds (UVACs) for protection against UV radiation. To assess whether the same strategy applies to sea ice-associated algal communities, MAAs were measured in algae associated with surface melt ponds, sea ice, sea ice−water interface, and underlying seawater in a coastal bay of the Canadian Arctic Archipelago during the 2011 spring melt transition. Six UVACs were detected as the spring melt progressed, namely shinorine, palythine, and porphyra-334 and three unknowns (U1, U2 and U3). U1 was most likely palythene, another MAA. The molecular identities of the other two UVACs, U2 and U3, which have an absorption maximum of 363 and 300 nm, respectively, remain to be structurally elucidated. The results confirm that Arctic sea ice-associated algal communities are capable of producing photoprotectants and that spatial and temporal variations in MAA and other UVAC synthesis are affected by snow cover and UV radiation exposure.

Acknowledgements

I would like to thank my supervisor Dr. Feiyue Wang for his support, encouragement and guidance through the development of this work. I greatly appreciate the opportunities I was awarded throughout my graduate studies.

I would also like to thank my co-supervisor Dr. C. J. Mundy for his advice and guidance through this research endeavor.

I would like to thank Dr. John Sorensen and Dr. Mark Hanson, my graduate committee members, for their time, collaboration and advice throughout my thesis work.

A special thanks to Dr. Charles Wong and Jennifer Low who were integral in preparing me for graduate studies and whom without I would not be successful. Thanks to Debbie Armstrong for her expertise advice and support throughout this research endeavor.

To my partner, Michael, and my children, Anders and Nolan, thank you for your patience and being my constant source of joy. To my parents, thank you for your years of dedication, encouragement and support.

Dedication

For Nana and Grammy.

My debt to you is immeasurable.

It takes a village to raise children and you have been my village.

I could not have done it without you.

Table Of Contents

List of Figures

List of Tables

List Of Copyrighted Material

List Of Abbreviations

ADME: adamantly function group
CDOM: chromophoric dissolved organic carbon
Chl *a*: chlorophyll *a*
CFCs: chlorofluorocarbons
CPDs: cyclobutane pyrimidine dimers
DAD: diode array detector
DNA: deoxyribose nucleic acid
ESI: electrospray ionization
FSW: 0.2 µm filtered seawater
FYI: first year sea ice
GFF: glass fiber filter
HPLC: high performance liquid chromatography
MAA: Mycosporine-like amino acid
mAU: milli absorbance units
MCAL: Manitoba Chemical Analysis Laboratory
MRM: multiple reaction monitoring
MS: mass spectrometer
MYI: multi-year sea ice
NMR: nuclear magnetic resonance
PAR: photosynthetically active radiation
ROS: reactive oxygen species
U1: unknown UV-absorbing compound with an absorbance maxima at 358 nm; suspected to be palythene
U2: unknown UV-absorbing compound with an absorbance maxima at 363 nm and 337 nm
U3: unknown UV-absorbing compound with an absorbance maxima at 300 nm
UCTEL: Ultra-Clean Trace Elements Laboratory
UV: ultraviolet
UVA: UV radiation between the wavelengths 315-400 nm
UVAC: UV-absorbing compound
UVB: UV radiation between the wavelengths 280-315 nm
UVC: UV radiation wavelengths less than 280 nm
UVR: Ultraviolet radiation
ΣUVAC: calculated as the sum of shinorine, palythine, porphyra-334 and U1-U3
ΣUVAC*: ΣUVAC relative to the total algal biomass measured as chl *a*

Chapter 1: Introduction

Despite its separation from dense human populations the Arctic has shown to be more sensitive to the impact of climate change than more temperate locations. The Arctic environment is a complex system where many feedback mechanisms exist, such as the ice-albedo effect, which make it particularly vulnerable to accelerated rates of warming (ACIA, 2004). It is estimated that the average temperature increase in the Arctic is 2 to 3 times greater then the global rate of change (ACIA, 2004). The rate of decreasing sea ice extent has increased from -2.2 to -3.0% per decade in 1979 to -10.1 to -10.7% per decade in the past 10 years (Comiso et al., 2008). This is coupled with increases in the frequency of stratospheric ozone depletion events, which were previously only thought to be prevalent in the Antarctic region (Manney et al., 2011). These changes may have an impact on the exposure of ultraviolet radiation (UVR) to organisms within the region, which can affect ecosystem functioning. Marine phytoplankton are known to produce mycosporine-like amino acids (MAAs) for protection against UVR. This thesis investigates the presence of MAAs in algae associated with an Arctic landfast sea ice cover. Algae are the main source of primary production in the marine ecosystems where in the Arctic, a significant portion of the total annual production can occur associated with a sea-ice cover (Leu et al., 2015). This thesis research will aid in the understanding of the ability of ice-associated algae to cope with changing light conditions in the Arctic.

1.1 Sea Ice-Associated Algae

In most marine ecosystems phytoplankton is the main source of primary production. In the permanently ice-covered Arctic Ocean, algae associated with sea ice are the main source of primary production (Gosselin et al., 1997). Four communities have been defined based on their

vertical profile within the sea ice: surface, interior, bottom, and sub-ice communities (defined by (Horner et al., 1992)) as well as a fifth under-ice melt pond community (defined by (Gradinger, 1996)).

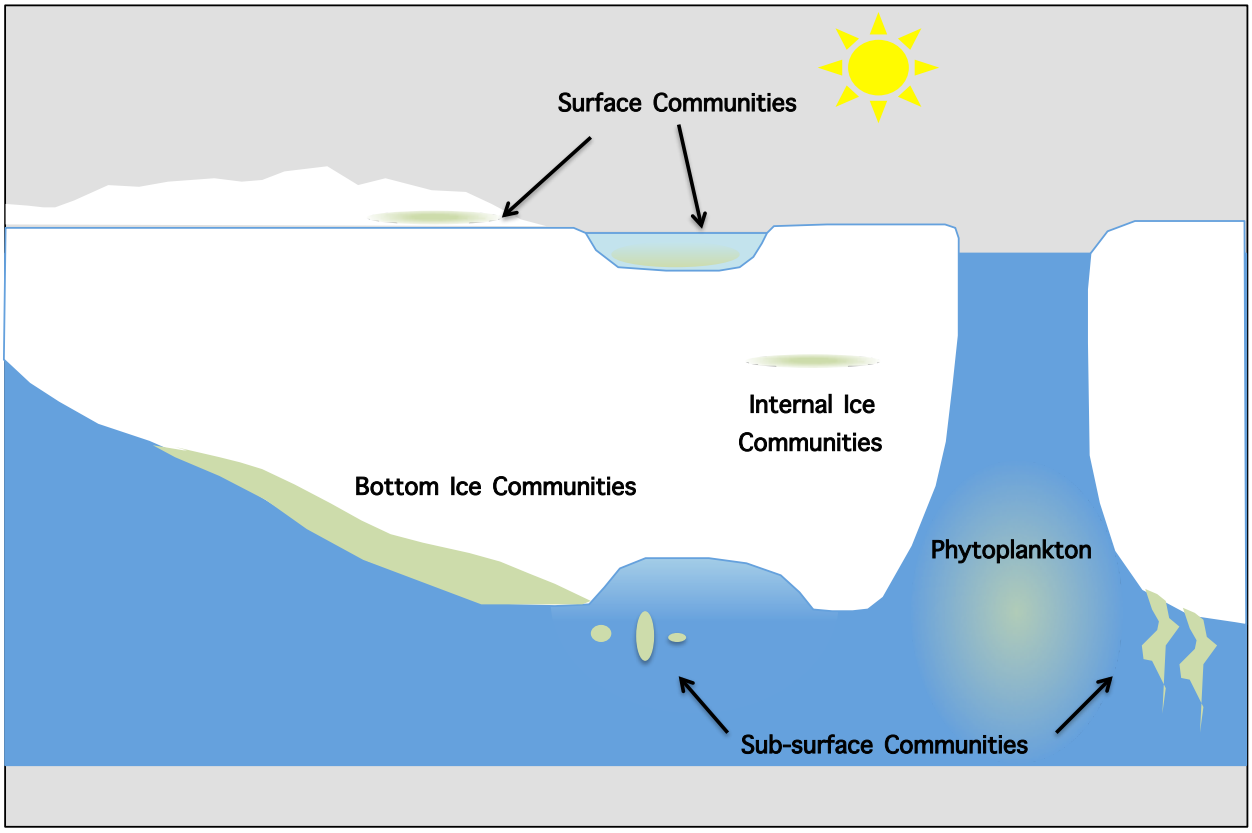

Figure 1.1 Illustration describing the location of typical algal communities (green) associated with sea ice.

The surface ice community (Figure 1.1) is contained within the frazil ice layer, which is the uppermost region of the ice that is formed first during sea ice growth. Algae from the water column are scavenged by forming ice particles and entrained. The entrained cells are under very harsh conditions such as high salinity (in brine channels), low temperatures and limited nutrients. The development of a productive community is dependent on the influx of nutrients, typically from seawater that is flooded onto the ice surface. Surface flooding is more common in Antarctic sea ice where snow depths on top of the ice frequently become so great that the ice becomes

depressed beneath the seawater surface. Seawater can also infiltrate the ice surface when ice floes converge in rafting events. Productive communities resulting from surface flooding are more common in the Antarctic and can last several weeks before melting (Garrison et al., 1986; Kattner et al., 2004).

Surface melt pond communities (Figure 1.1) are seeded from the algae cells that are contained in the frazil ice layer. It is present during the late stages of sea ice melt when melt ponds are present while there is some connection to a nutrient supply, typically in June-July in the Canadian Arctic (Bursa, 1963; Mundy et al., 2011). The species of algae that develop in these ponds may include flagellate, dinoflagellate, centric and pennate diatoms as well as ciliate species (Bursa, 1963; Elliott et al., 2015).

High brine salinities and low temperatures often prevent metabolic activity of algae cells within the upper sections of sea ice (Arrigo and Sullivan, 1992). Development of these organisms depends on access to nutrients within the narrow brine channels, which typically do not exchange with the seawater below at low temperatures (Golden et al., 2007). Presence of internal ice algal communities (Figure 1.1) can develop at the freeboard level where seawater may infiltrate in cavities or other structures. This type of community is more commonly found in Antarctic sea ice (Hegseth and Von Quillfeldt, 2002). Algae present are typically pennate and centric diatom species as well as flagellate species (Hegseth and Von Quillfeldt, 2002; Mundy et al., 2011).

The bottom ice community (Figure 1.1) is the most dominant and productive community in sea ice-covered oceans. The organisms inhabiting the bottom few centimeters of sea ice have an advantage of being suspended in the upper ocean, within close proximity to sunlight, as well as inhabiting a porous area of the ice that is in continuous exchange with the underlying

seawater. Pennate diatom genera such as *Nitzchia, Fragilariopsis* and *Navicula* species dominate this community (Poulin et al., 2011). The large diatom cells (>20 μm) are an important source of organic carbon for Arctic plankton and benthos during periods of ice melt (Gradinger and Bluhm, 2009; Michel et al., 2006; Michel et al., 1996).

Sub-surface communities (Figure 1.1) include three types, suspended, aggregate and under-ice melt communities, which are associated with the sea ice, but within the water column environment. Both aggregate species and under-ice melt communities are associated with the sea ice from their origins, while the suspended communities are physically adhered to the ice bottom. *Melosira arctica* is a centric diatom species that is common beneath multiyear ice (Melnikov et al. 2002; Fernadez-Mendez et al. 2014)—less common but present in first-year ice (Poulin et al. 2014)—and forms strands beneath the ice. Suspended communities are often formed when bottom ice communities are sloughed off during the spring melt transition. The under-ice melt community (Figure 1.1) contains a mixing between phytoplankton species, bottom ice aggregates and surface melt pond communities (Apollonio, 1985; Elliott et al., 2015; Gradinger, 1996; Mundy et al., 2011). The under-ice melt occurs in areas beneath melt ponds due to the increase in light transmission and absorption (Eicken et al., 2002), as well as heat conduction from pooled surface drained melt water. In the late stages of melt the ice becomes increasingly porous and surface melt water can percolate through the ice allow mixing between the bottom and surface communities.

Sea ice-associated algae inhabit an environment that is undergoing rapid change due to anthropogenic influences. One such change is the light regime that they are experiencing and will experience in the future.

1.2 Changing Light Conditions in the Arctic

1.2.1 Radiative Transfer of UVR through Air, Water and Ice

The transfer of radiation through a medium is dependent on the scattering and absorption properties of the medium. The exposure of marine organisms to UVR is dependent on the Sun angle—a function of latitude—followed by reflection and transmission through the Earth's atmosphere, snow and sea ice cover if present, the water column and ultimately into the individual cell where it can influence physiological functions. Therefore, there are many factors that affect the intensity of UVR exposure to marine organisms.

For instance the angle at which radiation travels relative to a line perpendicular to the earth's surface affects light transmission. This angle is referred to as the zenith angle. At greater zenith angles the energy from the Sun is spread over a larger area, resulting in smaller irradiances (W m^{-2}). A greater zenith angle also increases the atmospheric path length that the light must travel. Therefore when the Sun is directly above the Earth and the zenith angle is small, greater light intensities will be experienced.

Once UVR reaches the Earth's surface it must be transmitted through the water column to reach marine organisms. The amount of light transmitted depends primarily on absorption by water, chromophoric dissolved organic matter (CDOM) and particulate matter (including algae) within the water column. A water body with high productivity will therefore have greater amounts of absorbing particulates and CDOM and low transmission of UVR. Oligotrophic (nutrient poor - low productivity) waters will typically contain low concentrations of absorbing particulates and CDOM and have higher transmission of UVR.

The transfer of radiation into marine environments in Polar Regions is further influenced by the presence of snow-covered sea ice. The amount of UVR above and beneath a sea ice cover

is influenced by surface conditions, scattering and absorption in the snow and sea ice, snow depth, ice thickness and inclusions within the sea ice (Thomas and Dieckmann, 2009). Snow, for example, can greatly affect albedo and causes light to be diverted away from the underlying water column. In regions that have a seasonal ice cover, the sea ice melt transition marks a time of rapid change in light conditions for marine organisms. As snow melts from the sea ice surface there is an increase in UVR transmission to the ice due to a decreasing albedo and light attenuating layer. Following snowmelt, the ice surface quickly warms causing the formation of melt ponds across sea ice; this further increases light transmission to the underlying water column. The transmission of UVR is approximately 10-times greater through melt ponds than bare ice (Perovich, 2006). This is due to a low albedo and high transparency of melt water to UVR versus those of an adjacent drained white ice cover.

1.2.2 Stratospheric Ozone

Stratospheric ozone is responsible for the absorption of a large fraction of solar UVR before it reaches the surface environment. Ozone formation and destruction in the stratosphere occur naturally through photochemical reactions. Molecular oxygen (O_2) absorbs short-wavelength UVR from the Sun and is broken down into atomic oxygen. The very reactive atomic oxygen then reacts with surrounding molecular oxygen to form ozone. The so-formed ozone can also be photolytically decomposed into molecular oxygen and atomic oxygen. The rate of formation of ozone is greater than the rate of destruction in the stratosphere, allowing for the accumulation of ozone at that altitude (Wayne 1991). However, anthropogenic chemicals such as chlorofluorocarbons (CFCs) can be transported to the stratosphere where they produce chlorine radicals and catalyze the decomposition of ozone at a rate that cannot be replenished naturally. The most severe stratospheric ozone depletion, known as “ozone holes”, has been observed

during the springtime over the Antarctica since the 1980s, raising major concerns over the increasing intensity of solar UVR reaching the surface environment (Farmer et al., 1987). Although the situation has been alleviated with the signing of the Montreal Protocol in 1987 phasing out some of the ozone-depleting chemicals, springtime stratospheric ozone depletion has been a reoccurring phenomenon over the Antarctica due to the long half-lives of CFCs (Chatterjee 1995).

Stratospheric ozone depletion can also occur over the Arctic, although to a lesser severity and frequency. During the springtime of 2011 an unprecedented stratospheric ozone depletion event was observed in the Arctic (Manney et al., 2011). This event was considered to be the first observation of an ozone hole in this region that compared to the depletion of ozone (>80% depletion at 18-20 km altitude) observed in the Antarctic region (Manney et al., 2011). The conditions surrounding this event that caused such an extreme reduction in ozone are a prolonged cold period in the lower stratosphere and a strong polar vortex (Bernhard et al., 2013). Ultraviolet radiation intensities greatly increased in 2011, in conjunction with the reduction of ozone, exceeding the climatological mean by 77% in Alaska, Greenland, Canada and 161% in Scandinavia (Bernhard et al., 2013). Although not occurring on an annual basis, data have shown that there have been increases in the frequency of stratospheric ozone depletion events over the Arctic in recent years (Manney et al. 2011). The effect of the formation of an ozone hole on biota in the Arctic has not yet been evaluated. However, extensive studies have been done in the Antarctic region and can be used as a starting point for how ice-associated organisms may respond to changes in concentrations of stratospheric ozone. As expected research has shown that the response to increased UVR at the species level for Antarctic microalgae is highly

variable among species (Buma et al., 2006) and depends greatly on the light history of the organism.

1.2.3 Sea Ice Conditions

A significant decrease in the extent of perennial sea ice within the Arctic system (Kwok et al., 2009) is projected to continue until we see a markedly different ice regime in the region, mainly consisting of first-year sea ice (FYI) (Holland et al., 2006; Stroeve et al., 2007; Stroeve et al., 2014). FYI tends to be thinner and more saline than multiyear sea ice (MYI), resting closer to the sea level. Further the melt pond coverage during spring is much greater over FYI than MYI. Transmittance of shortwave radiation (250-2500 nm) through FYI (0.11) can be three times larger than through MYI (0.04) and the absorption can be doubled (Nicolaus et al., 2012). The transmission of light between the wavelengths of 400-700 nm (photosynthetically active radiation; PAR) is greatly increased through melt pond covered sea ice, up to 67% transmission as opposed to up to 16% through white ice (Ehn et al., 2011). Because of the continuity of absorption of light in ice between the wavelengths of 250-400 nm, it follows that in a FYI regime sea ice algae and phytoplankton beneath the sea ice will have a greater exposure to UVR.

1.2.4 Water Column Stratification

Climate change is also predicted to increase fresh water inputs from melting sea ice, glaciers and increases in river discharge. Freshwater inputs can increase stratification of the upper water column (Peterson et al., 2002). Primary producers within this upper stratified layer of the water column are at greater risk of UVB exposure because of a decrease in the surface mixed layer thickness. Buma et al. (2001) found that at times of increased stratification in the water column, there is greater DNA damage to organisms at the surface as opposed to times when there is greater mixing and DNA damage is more homogeneous throughout the upper

water column (Buma et al., 2001). This finding indicates that stratification of the water column prevents phytoplankton from mixing which can increase the overall exposure of UVB.

A primary concern is the timing of such events. The estimated rate of change for the onset of melt in the Arctic range from -1.0 d decade^{-1} to -7.0 d decade^{-1}, varying by region (Markus et al., 2009). If the spring melt transition continues to occur earlier in the year then it would be possible for this event to coincide with the peak ozone depletion event, which occurs in March-April. In such a case we would see the largest exposure of marine organisms to high levels of UVR and the greatest impact on the ecosystem.

1.3 Damaging Biological effects of UVR

The solar spectrum reaching the Earth's surface includes UVR (λ<400 nm emitted from the Sun) that can be divided into UVA (λ=315-400 nm), UVB (λ=280-315 nm) and UVC (λ<280 nm) bands. Although these bands of radiation contribute only a small fraction of the total incoming radiation (Figure 1.2), the higher energy at these shorter wavelengths can cause a disproportionate amount of damage to biological organisms (Caldwell, 1979) (Figure 1.2). Primary producers need to absorb and fix the Sun's energy into organic matter and therefore, they can be particularly vulnerable to changes in the intensity of incoming UVR. The ability to acclimate to UVR stress can vary greatly between species depending on their environmental exposure and photophysiology.

DNA damage from UVR is mainly due to the UVB band between the wavelengths of 290-320 nm (Figure 1.2). This is due to the ability of DNA to absorb radiation within this range resulting in the formation of DNA mutations. Cyclobutane pyrimidine dimers (CPDs) are the most common mutations and can be used as an indicator of UV-induced damage in a cell or organism (Buma et al., 2001; Buma et al., 2006). Damage to an organism's DNA can result in a

cascade of events that can be lethal to a cell. The formation of DNA dimers such as CPDs can disrupt normal cell functions such as DNA replication and transcription, leading to mutagenesis

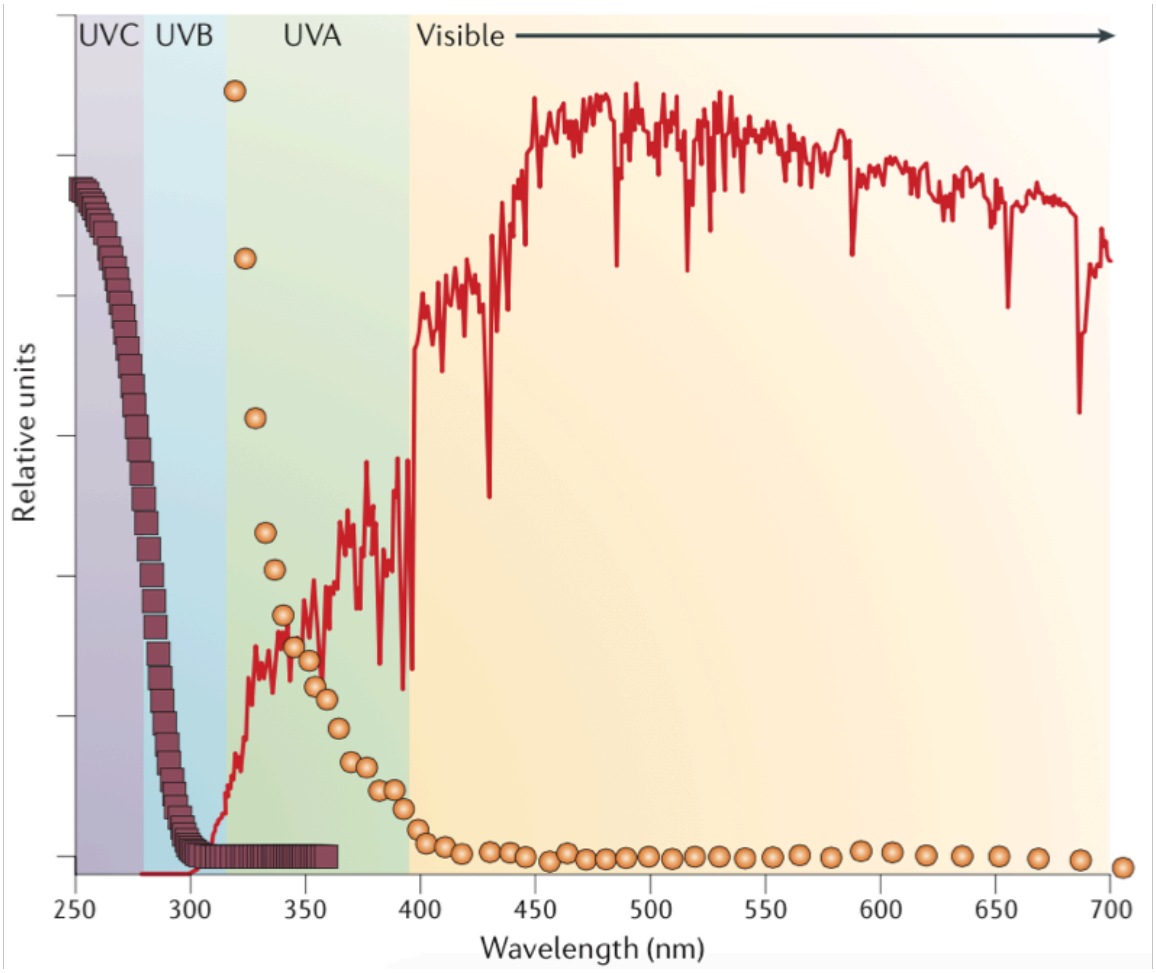

Figure 1.2 Adapted with permission from Gao et al. (Gao and Garcia-Pichel 2011). Standard solar spectrum reaching the Earth's surface (red line) and the action spectrum causing direct DNA damage to living cells (purple boxes) and inhibition of photosynthesis (yellow circle).

and cell death (Rastogi and Incharoensakdi, 2014). Double strand breaks are a direct result of attempts by the cell to replicate the DNA that contains lesions such as those described above.

Photosynthetic organisms that undergo aerobic metabolism are always at a threat of the oxygen in their environment that can oxidize important cellular components. High light conditions can cause increased formation of reactive oxygen species (ROS) through photosystem II (Latifi et al., 2009) where ROS are formed through the photosynthetic process. Reactive

oxygen species include oxygen radicals such as superoxide ($\bullet O_2$), hydroxyl radical ($\bullet OH$), peroxyl radical ($RO_2\bullet$), and hydroperoxyl radicals ($HO_2\bullet$) as well non-radical reactive oxygen species such as hydrogen peroxide (H_2O_2), hypochlorous acid (HOCl) and ozone (O_3). Increase in the production of ROS and oxidative stress induced by UVB has been measured in laboratory experiments using cyanobacteria cultures (He and Häder, 2002).

Photoinhibition, a decrease in photosynthetic capacity with increasing light exposure, is a result of the production of ROS and represents an indication of high light stress in photosynthetic organisms. Photoinhibition is observed under high photosynthetically active radiation as well as at low intensities of UVA and/or UVB radiation. A relationship can be seen between the extent of photoinhibition and the wavelength of radiation (Figure 1.2). Photoinhibition is caused by an active downregulation of the photosynthetic electron transport chain in photosystem II via degradation of the D1 protein. The extent to which cells experience photoinhibition is affected by the light history of the cell and the species composition of the community. Tropical phytoplankton have been shown to be more resilient to photoinhibition than polar phytoplankton communities (Helbling et al., 1992).

1.4 UVR protective strategies of algae

Strategies used by organisms to acclimate to elevated exposure of UVR include repair mechanism, avoidance, and production of secondary metabolites such as UVR screening molecules, outer sheath pigments and antioxidants (Wada et al., 2013).

1.4.1 DNA Repair Mechanisms

Research into the mechanisms of DNA repair has been focused primarily on understanding the complex repair mechanisms that occur within bacterial cells (*E. coli*) and human cells with the intention of understanding ourselves at the forefront. Cells contain

specialized proteins that scan the genome continuously for damage and trigger appropriate repair mechanisms when possible. In plant cells the two main pathways of DNA repair mechanisms that have been identified are photoreactivation and nucleotide excision repair (Britt, 2004). Photoreactivation is done through the use of photolyases that can repair the lesions that are most commonly encountered. Photolyases use light as an energy source in the visible/blue light band in order to reverse the DNA damage from UVB.

1.4.2 Avoidance

Avoidance of UVR is a general mechanism used by organisms to reduce exposure to UVR. Microorganisms may avoid UVR by motility mechanisms, mat forming capabilities or its distribution within a surface mix layer (Singh et al., 2010).

For some organisms, such as phytoplankton, exposure to UVR is dependent on the depth that the organism is present within the water column. The rate of mixing and the depth of the surface mixing layer impact the rate at which organisms accumulate damage from UVR. In highly stratified water systems organisms have a shallow surface mix layer and are continuously exposed to incident radiation (Buma et al., 2001). This can cause an accumulation of DNA damage due to limitations in the rate of DNA lesion repair. As such, some organisms capable of sensing and avoiding high levels of radiation will move away from high UVR using motility mechanisms (Quesada and Vincent, 1997).

1.4.3 Secondary Metabolites

Most organisms routinely divert resources from primary processes to produce secondary metabolites, molecules that are not essential for life, in order to reduce damage from external stresses in their environment. One example is the production of molecules for the prevention of damage from UVR. These molecules can be produced constitutively for some organisms, while

others will produce them only in response to an external stimulus, such as high UVR or high PAR. Antioxidants as well as UVR screening compounds are examples of such molecules.

High light condition can cause excessive energy to photoreactions increasing the production of ROS and is considered a by-product of UVR stress. Antioxidants can be used to mitigate damage caused by the production of ROS from UVR exposure. There are two main types of antioxidants used in microorganisms, non-enzymatic and antioxidant enzymes. Antioxidants function to quench ROS before they can interact with and damage important cellular components (Latifi et al., 2009).

In photosynthetic organisms mycosporine-like amino acids (MAAs) and scytonemin are used as UVR screening molecules. Scytonemin is a molecule that is produced exclusively by cyanobacteria and it is able to absorb UV-A light with an absorbance maximum of 386 nm (Singh et al., 2010). This pigment tints the external sheath of organisms containing it to a red-brown color. These pigments have been confirmed to increase in production in response to high light intensities (Garcia-Pichel and Castenholz, 1991). These molecules have been identified in Antarctic melt ponds (Garcia-Pichel and Castenholz, 1991), though they have yet to be observed in Arctic melt ponds.

The other type of UVR screening molecules are MAAs, which are the focus of this thesis research.

1.5 Mycosporine-like Amino Acids

MAAs are small molecular weight (<300 Da), UVR-absorbing compounds produced by a variety of organisms to protect them from detrimental effects of UVR (Shick and Dunlap, 2002). These molecules are unique in their ability to absorb UVR and remain relatively photostable due to their ability to

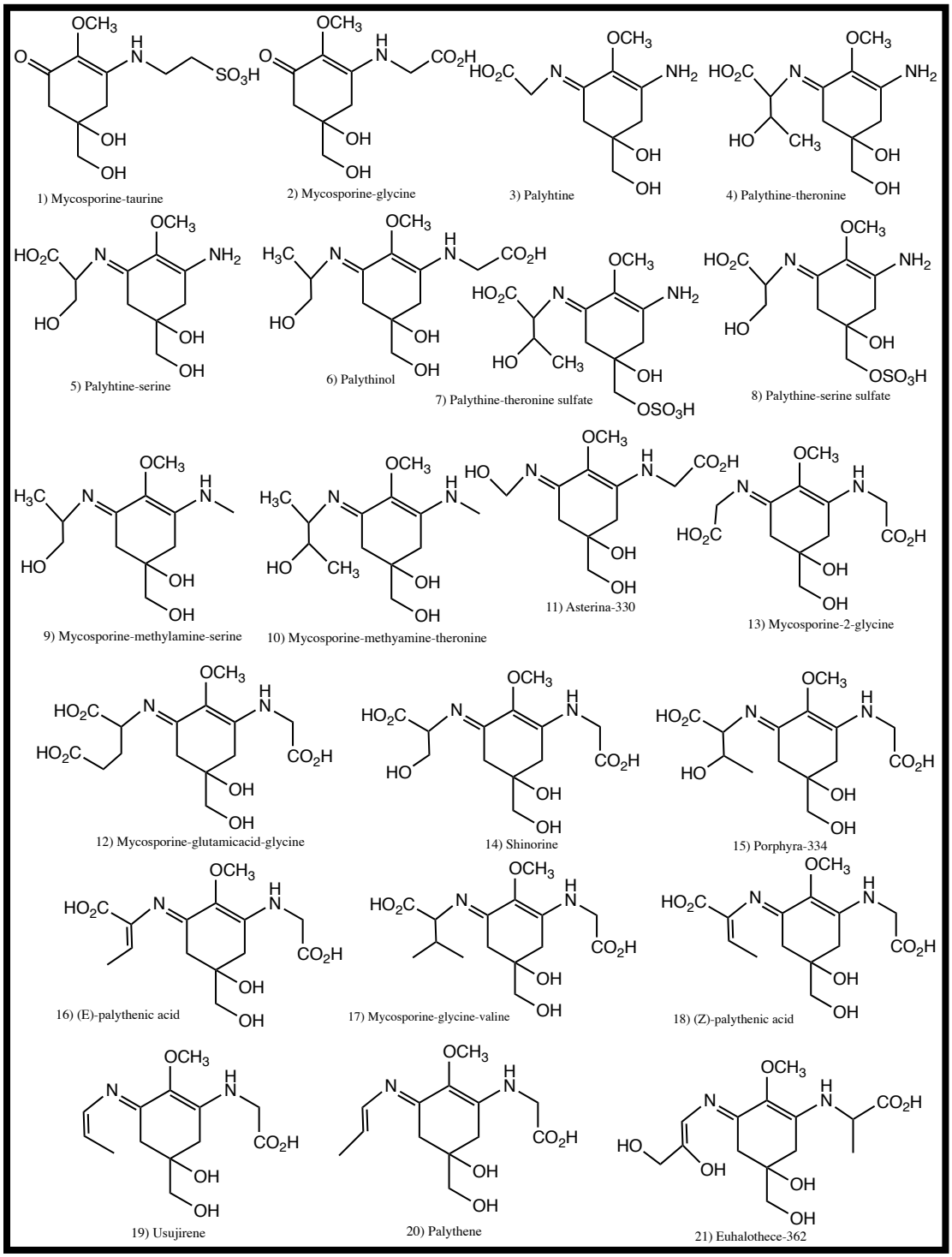

Figure 1.3 Molecular structures of mycosporine-like amino acids derived form natural sources.

dissipate the energy as heat into their surroundings (Conde et al., 2000). MAAs can also be involved in other functions such as antioxidation (Dunlap and Yamamoto,1995; Suh et al.,

2003), molecular repair (Shick and Dunlap, 2002) and osmotic regulation (Oren, 1997), which add to its role as a secondary metabolite to organisms who are capable of producing MAAs in some form. My thesis focuses on the use of MAAs for the protection of algal cells from the damaging effects of UVR.

In tropical and temperate oceans experiencing high intensity UVR, the ability to synthesize or acquire MAAs appears to be ubiquitous among marine phytoplankton (Shick and Dunlap, 2002), although only limited capabilities have been reported in pennate diatom species (Jeffrey et al., 1999).

Some very preliminary work has been done on investigating the presence of these metabolites in the Arctic region and within sea ice globally. So far MAAs have been identified in sea ice cores taken from the Baltic Sea (Piiparinen et al., 2015; Uusikivi et al., 2010), in the water column near Svalbard, Arctic (Ha et al., 2012) as well as in sea ice algae communities in the Antarctic (Ryan et al., 2002). The significance of these compounds to these communities remains unclear, although based on observational data, their role for UVR protection in Antarctic sea ice algae has been proposed to be negligible (Ryan et al., 2002). This suggestion may also hold true for Arctic ice algal communities; however, limited work has been done to properly address this conclusion. The diatom-dominated sea ice algae communities may be at a disadvantage to other organisms in these changing conditions if they are not able to protect themselves from increasing exposure to UVR.

1.5.1 Structures of MAAs

The precursor for MAAs is 4-deoxy-gadusol, which is biosynthesized through both the shikimate or pentose phosphate pathways (Spence et al., 2012). The addition of amino acids, amino alcohols and other amino groups results in the formation of a variety of MAAs, over 20 of

which have been structurally elucidated (Carreto and Carignan, 2011). The variability in MAA structures (Figure 1.3) is thought to be produced by embarking small changes to the later steps in the biosynthetic pathway. Organisms are also thought to be capable of converting MAAs from one form to another in response to changes in the environmental conditions. Structural diversity is complex and includes MAAs that contain sulfate esters (structures 7, 8 in Figure 1.3). In cyanobacteria, MAAs have been reported to be covalently linked to oligosaccharides (Böhm et al., 1995). Atypical compounds containing more than one absorption maximum have also been tentatively characterized as esters formed by the condensation of two MAAs (Carreto et al., 2001).

1.5.2 Spectral Properties of MAAs

Absorption maxima (λ_{max}) and extinction coefficients (ε) of MAAs are determined primarily by the nature of the groups linked to the amino-cyclohexenimine ring as well as the composition of the surrounding environment. The characteristic strong absorption band is observed within the UVA range (λ_{max} between 310-360 nm, Table 1.1); this is the energy required to delocalize electrons present within the conjugated double bond system. There are many structural changes that can cause differences in the observed absorption maxima (Table 1.1, Figure 1.3). A bathochromic (higher wavelength, lower frequency) shift in the λ_{max} is seen as the π electron distribution over the molecule increases (Table 1.1). For example mycosporine-glycine (structure 2, Figure 1.3) contains two conjugated double bonds and has a λ_{max} of 310 nm, while palythene (structure 20, Figure 1.3) contains three conjugated double bonds and its λ_{max} shifted to 356 nm. The extinction coefficient describes the efficiency of the electron delocalization in the molecule, therefore, a higher molar extinction coefficient describes a

Table 1.1 Spectral properties and molar mass of common mycosporine-like amino acids. Corresponding structures can be seen in Figure 1.3. Absorption maxima were taken from Carreto and Carignan 2011. Extinction coefficients were obtained from two sources (1) (Gröniger et al., 2000) and (2) (Dunlap and Shick, 1998)

I.D.	Name	Maximum Absorbance (nm)	Extinction Coefficient ($M\ cm^{-1}$)	Molar Mass ($g\ mol^{-1}$)
1	Mycosporine-taurine	310		295
2	Mycosporine-glycine	310		245
3	Palythine	320	36200 (2)	244
4	Palythine-threonine	320		288
5	Palythine-serine	320		274
6	Palythinol	320	43500 (2)	302
7	Palythine-threonine sulfate	321		367
8	Palythine-serine sulfate	321		354
9	Mycosporine-methylamine-serine	325		288
10	Mycosporine-methylamine-theronine	330		302
11	Asterina-330	330	43500 (1)	288
12	Mycosporine-glutamicacid-glycine	330		375
13	Mycosporine-2-glycine	332		302
14	Shinorine	333	44700 (1)	332
15	Porphyra-334	334	42300 (1)	346
16	(E)-palythenic acid	335		329
17	Mycosporine-glycine-valine	335		345
18	(Z)-palythenic acid	337		329
19	Usujirene	357		284
20	Palythene	360	50000 (2)	284
21	Euhalothece-362	362		331

molecule that is more efficient at absorbing light. Zhang et al. (2005) studied the effect of pH and temperature on the absorption maxima and extinction coefficient of porphyra-334, a common MAA. Their study revealed that the absorption maximum was fairly stable at ambient pH (4-12) and a hypsochromic shift (2-4 nm) occurred under highly acidic conditions (pH = 1-3). It was also noted that at lower pH there was a slight decrease in the extinction coefficient of the molecule. Temperature increases led to a decrease in absorption over time due to decomposition of porphyra-334 in the study.

1.5.3 Methods for Separation and Detection of MAAs

Several methods have been developed for the separation of MAAs using reverse phase high performance liquid chromatography (HPLC). Modification and innovation has primarily

been driven by the increasing number of MAAs observed and the need for increased resolution between MAAs with similar chemical properties. The mobile phases used are primarily acidified aqueous solution with different fractions of methanol and acetonitrile. Carreto et al. (2005) demonstrated the greatest capability to separate a variety of naturally occurring MAAs in one method. This method has not become the standard for most applications because of its length (55 minutes per sample) and its limited applicability to mass spectrometry (aqueous mobile phase), which has become increasingly popular for detection purposes.

Quantification of MAAs has been limited due to the lack of commercially available standards. Estimates of concentration have been based on the absorption using measured extinction coefficients (Table 2.1). Also without authentic standards, identification of MAAs has been, until more recently, primarily based off of published retention times and spectral properties. Identification without further evidence must be approached with caution due to the high number of MAAs currently known, some with very similar structures, as well as the many new MAAs that are constantly being identified.

1.6 Organization of This Thesis

The goal of my thesis research is to contribute to our understanding of the ability of sea ice-associated algal communities to tolerate changes in UVR exposure. It is not well understood if organisms that are adapted to typically low light conditions would retain the capacity to produce compounds such as MAAs to provide protection in high UVR conditions. To satisfy this goal our objectives are to identify the MAAs present in sea ice-associated algal communities, as well as to determine their spatial and temporal evolution.

This thesis is a sandwich style thesis containing 4 chapters. Chapter 1 (this chapter) provides a context that is pertinent to the thesis research. Chapter 2 describes the presence of

MAAs in a sea ice community in the Canadian Arctic; the chapter has been recently published in *Marine Ecology Progress Series* (Elliott et al., 2015). Chapter 3 describes efforts towards developing a method for the isolation of a novel UV-absorbing compound encountered in melt pond communities as reported in Chapter 2. Chapter 4 provides a conclusion to the thesis and describes our thoughts on the most logical steps forward in this research area.

Literature cited

ACIA E (2004) Impacts of a Warming Arctic-Arctic Climate Impact Assessment (ACIA) by Arctic Climate Impact Assessment 144 ISBN 0521617782 Cambridge, UK: Cambridge University Press, December 2004 1042p

Apollonio S (1985) Arctic Marine Phototrophic Systems: Functions of Sea Ice Stabilization. Arctic 38:167-173

Arrigo KR, Sullivan CW (1992) The influence of salinity and temperature covariation on the photophysiological characteristics of antarctic sea ice microalgae. J Phycol 28:746-756

Bernhard G, Dahlback A, Fioletov V, Heikkila A, Johnsen B, Koskela T, Lakkala K, Svendby T (2013) High levels of ultraviolet radiation observed by ground-based instruments below the 2011 Arctic ozone hole. Atmos Chem Phys 13:10573-10590

Böhm GA, Pfleiderer W, Böger P, Scherer S (1995) Structure of a Novel Oligosaccharide-Mycosporine-Amino Acid Ultraviolet A/B Sunscreen Pigment from the Terrestrial Cyanobacterium Nostoc commune. Journal of Biological Chemistry 270:8536-8539

Britt AB (2004) Repair of DNA damage induced by solar UV. Photosynthesis Research 81:105-112

Buma AGJ, De Boer MK, Boelen P (2001) Depth distributions of DNA damage in Antarctic marine phyto- and bacterioplankton exposed to summertime UV radiation. J Phycol 37:200-208

Buma AGJ, Wright SW, Enden Rvd, Poll WHvd, Davidson AT (2006) PAR acclimation and UVBR-induced DNA damage in Antarctic marine microalgae. Mar Ecol-Prog Ser 315:33-42

Bursa A (1963) Phytoplankton in Coastal Waters of the Arctic Ocean at Point Barrow, Alaska. Arctic 16:239-262

Caldwell MM (1979) Plant Life and Ultraviolet Radiation: Some Perspective in the History of the Earth's UV Climate. BioScience 29:520-525

Carreto JI, Carignan MO (2011) Mycosporine-Like Amino Acids: Relevant Secondary Metabolites. Chemical and Ecological Aspects. Mar Drugs 9:387-446

Carreto JI, Carignan MO, Montoya NG (2001) Comparative studies on mycosporine-like amino acids, paralytic shellfish toxins and pigment profiles of the toxic dinoflagellates Alexandrium tamarense, A. catenella and A. minutum. Mar Ecol-Prog Ser 223:49-60

Chatterjee k (1995) Implications of Montreal Protocol: with particular reference to India and other developing countries. Atmos Environ 29:1883-1903

Comiso JC, Parkinson CL, Gersten R, Stock L (2008) Accelerated decline in the Arctic sea ice cover. Geophys Res Lett 35

Conde FR, Churio MS, Previtali CM (2000) The photoprotector mechanism of mycosporine-like amino acids. Excited-state properties and photostability of porphyra-334 in aqueous solution. J Photochem Photobiol B-Biol 56:139-144

Dunlap WC, Shick JM (1998) Ultraviolet radiation-absorbing mycosporine-like amino acids in coral reef organisms: A biochemical and environmental perspective. J Phycol 34:418-430

Dunlap WC, Yamamoto Y (1995) Small-molecule antioxidants in marine organisms: Antioxidant activity of mycosporine-glycine. Comp Biochem Physoil 112:105-114

Ehn JK, Mundy CJ, Barber DG, Hop H, Rossnagel A, Stewart J (2011) Impact of horizontal spreading on light propagation in melt pond covered seasonal sea ice in the Canadian Arctic. J Geophys Res-Oceans 116

Eicken H, Krouse H, Kadko D, Perovich D (2002) Tracer studies of pathways and rates of meltwater transport through Arctic summer sea ice. J Geophys Res-Oceans 107
Elliott A, Mundy CJ, Gosselin M, Poulin M, Campbell K, Wang F (2015) Spring production of mycosporine-like amino acids and other UV-absorbing compounds in sea ice-associated algae communities in the Canadian Arctic. Mar Ecol-Prog Ser 541:91-104
Farmer, CB, Toon, GC, Schaper PW, Blavier JF, Lowes LL (1987) Stratospheric trace gases in the spring 1986 Antarctic atmosphere. Nature 329:126-130
Gao Q, Garcia-Pichel F (2011) Microbial ultraviolet sunscreens. Nature 11:791-802
Garcia-Pichel F, Castenholz RW (1991) Characterization and biological implications of scytonemin, a cyanobacterial sheath pigment. J Phycol 27:395-409
Garrison DL, Sullivan CW, Ackley SF (1986) Sea Ice Microbial Communities in Antarctica. BioScience 36:243-250
Golden KM, Eicken H, Heaton AL, Miner J, Pringle DJ, Zhu J (2007) Thermal evolution of permeability and microstructure in sea ice. Geophys Res Lett 34
Gosselin M, Levasseur M, Wheeler PA, Horner RA, Booth BC (1997) New measurements of phytoplankton and ice algal production in the Arctic Ocean. Deep-Sea Res Part II-Top Stud Oceanogr 44:1623
Gradinger R (1996) Occurrence of an algal bloom under Arctic pack ice. Mar Ecol-Prog Ser 131:301-305
Gradinger R, Bluhm B (2009) Timing of Ice Algal Grazing by the Arctic Nearshore Benthic Amphipod Onisimus litoralis. Arctic 63:355-358
Gröniger A, Sinha RP, Klisch M, Hader DP (2000) Photoprotective compounds in cyanobacteria, phytoplankton and macroalgae - a database. J Photochem Photobiol B-Biol 58:115-122
Ha S-Y, Kim Y-N, Park M-O, Kang S-H, Kim H-C, Shin K-H (2012) Production of mycosporine-like amino acids of in situ phytoplankton community in Kongsfjorden, Svalbard, Arctic. J Photoch Photobio B 114:1-14
He Y-Y, Him Y-N, Park M-O, Kang S-H, Kim H-C, Shin K-H (2012) Production of mycosporine-like amino acids of in situ phytoplankton c: protective effects of ascorbic acid and N-acetyl-l-cysteine. J Photoch Photobio B 66:115-124
Hegseth EN, Von Quillfeldt CH (2002) Low phytoplankton biomass and ice algal blooms in the Weddell Sea during the ice-filled summer of 1997. Antarct Sci 14:231-243
Helbling EW, Villafane V, Ferrario M, Holmhansen O (1992) Impact of natural ultraviolet-radiation on rates of photosynthesis and on specific marine-phytoplankton species. Mar Ecol-Prog Ser 80:89-100
Holland MM, Bitz CM, Tremblay B (2006) Future abrupt reductions in the summer Arctic sea ice. Geophys Res Lett 33
Horner R, Ackley SF, Dieckmann GS, Gulliksen B, Hoshiai T, Legendre L, Melnikov IA, Reeburgh WS, Spindler M, Sullivan CW (1992) Ecology of sea ice biota 1. Habitat, terminology, and methodology. Polar Biol 12:417-427
Jeffrey SW, MacTavish HS, Dunlap WC, Vesk M, Groenewoud K (1999) Occurrence of UVA- and UVB-absorbing compounds in 152 species (206 strains) of marine microalgae. Mar Ecol-Prog Ser 189:35-51
Kattner G, Thomas DN, Haas C, Kennedy H, Dieckmann GS (2004) Surface ice and gap layers in Antarctic sea ice: highly productive habitats. Mar Ecol-Prog Ser 277:1-12
Kwok R, Cunningham GF, Wensnahan M, Rigor I, Zwally HJ, Yi D (2009) Thinning and volume loss of the Arctic Ocean sea ice cover: 2003–2008. J Geophys Res-Oceans 114

Latifi A, Ruiz M, Zhang CC (2009) Oxidative stress in cyanobacteria. Fems Microbiol Rev 33:258-278
Leu E, Mundy CJ, Assmy P, Campbell KL, Gabrielsen TM, Gosselin M, Juul-Pedersen T, Gradinger R (2015) Arctic spring awakening - Steering principles behind the phenology of vernal ice algae blooms. Prog Oceanogr 139:151-170
Manney GL, Santee ML, Rex M, Livesey NJ, Pitts MC, Veefkind P, Nash ER, Wohltmann I, Lehmann R, Froidevaux L, Poole LR, Schoeberl MR, Haffner DP, Davies J, Dorokhov V, Gernandt H, Johnson B, Kivi R, Kyro E, Larsen N, Levelt PF, Makshtas A, McElroy CT, Nakajima H, Parrondo MC, Tarasick DW, von der Gathen P, Walker KA, Zinoviev NS (2011) Unprecedented Arctic ozone loss in 2011. Nature 478:469-465
Markus T, Stroeve JC, Miller J (2009) Recent changes in Arctic sea ice melt onset, freezeup, and melt season length. J Geophys Res-Oceans 114
Michel C, Ingram R, Harris L (2006) Variability in oceanographic and ecological processes in the Canadian Arctic Archipelago. Prog Oceanogr 71:379-401
Michel C, Legendre L, Ingram R, Gosselin M, Levasseur M (1996) Carbon budget of sea-ice algae in spring: evidence of a significant transfer to zooplankton grazers. J Geophys Res – All series 101
Mundy CJ, Gosselin M, Ehn JK, Belzile C, Poulin M, Alou E, Roy S, Hop H, Lessard S, Papakyriakou TN, Barber DG, Stewart J (2011) Characteristics of two distinct high-light acclimated algal communities during advanced stages of sea ice melt. Polar Biol 34:1869-1886
Nicolaus M, Katlein C, Maslanik J, Hendricks S (2012) Changes in Arctic sea ice result in increasing light transmittance and absorption. Geophys Res Lett 39
Oren A (1997) Mycosporine-like amino acids as osmotic solutes in a community of halophilic cyanobacteria. Geomicrobio J 14:231-240
Perovich DK (2006) The interaction of ultraviolet light with Arctic sea ice during SHEBA. Annals of Glaciology 44:47-52
Peterson BJ, Holmes RM, McClelland JW, Vörösmarty CJ, Lammers RB, Shiklomanov AI, Shiklomanov IA, Rahmstorf S (2002) Increasing River Discharge to the Arctic Ocean. Science 298:2171-2173
Piiparinen J, Enberg S, Rintala J-M, Sommaruga R, Majaneva M, Autio R, Vahatalo AV (2015) The contribution of mycosporine-like amino acids, chromophoric dissolved organic matter and particles to the UV protection of sea-ice organisms in the Baltic Sea. Photochem Photobiol Sci 14:1025-1038
Poulin M, Daugbjerg N, Gradinger R, Ilyash L, Ratkova T, von Quillfeldt C (2011) The pan-Arctic biodiversity of marine pelagic and sea-ice unicellular eukaryotes: a first-attempt assessment. Mar Biodivers 41:13-28
Quesada A, Vincent W (1997) Strategies of adaptation by Antarctic cyanobacteria to ultraviolet radiation. Eur J Phycol 32:335-342
Rastogi RP, Incharoensakdi A (2014) Characterization of UV-screening compounds, mycosporine-like amino acids, and scytonemin in the cyanobacterium Lyngbya sp CU2555. FEMS Microbiol Ecol 87:244-256
Ryan KG, McMinn A, Mitchell KA, Trenerry L (2002) Mycosporine-like amino acids in Antarctic sea ice algae, and their response to UVB radiation. Z Naturforsch C 57:471-477

Shick JM, Dunlap WC (2002) Mycosporine-like amino acids and related gadusols: Biosynthesis, Accumulation, and UV-Protective Functions in Aquatic Organisms. Annu Rev Physiol 64:223-262
Singh SP, Häder D-P, Sinha RP (2010) Cyanobacteria and ultraviolet radiation (UVR) stress: Mitigation strategies. Ageing Res Rev 9:79-90
Spence E, Dunlap WC, Shick JM, Long PF (2012) Redundant Pathways of Sunscreen Biosynthesis in a Cyanobacterium. ChemBioChem 13:531-533
Stroeve J, Holland MM, Meier W, Scambos T, Serreze M (2007) Arctic sea ice decline: Faster than forecast. Geophys Res Lett 34
Stroeve J, Markus T, Boisvert L, Miller J, Barrett A (2014) Changes in Arctic melt season and implications for sea ice loss. Geophys Res Lett 41:1216-1225
Suh HJ, Lee HW, Jung J (2003) Mycosporine glycine protects biological systems against photodynamic damage by quenching singlet oxygen with a high efficiency. Photochem Photobiol 78:109-113
Thomas DN, Dieckmann GS (2009) Sea Ice. Wiley
Uusikivi J, Vahatalo AV, Granskog MA, Sommaruga R (2010) Contribution of mycosporine-like amino acids and colored dissolved and particulate matter to sea ice optical properties and ultraviolet attenuation. Limnol Oceanogr 55:703-713
Wada N, Sakamoto T, Matsugo S (2013) Multiple roles of photosynthetic and sunscreen pigments in cyanobacteria focusing on the oxidative stress. Metabolites 3:463-483
Wayne R P (1991) Chemistry of the atmospheres: An introduction to the chemistry of the atmospheres of Earth, the Planets and their satellites. 2nd Edition. Oxford

Chapter 2: Spring Production Of Mycosporine-Like Amino Acids And Other UV-Absorbing Compounds In Sea Ice-Associated Algae Communities In The Canadian Arctic

This paper has been published in *Marine Ecology Progress Series.* The work represents a core chapter of my thesis. As the first author, I was primarily responsible for the methodological development, sample analysis, data processing and manuscript writing.

Elliott A, Mundy CJ, Gosselin M, Poulin M, Campbell K, and Wang F. (2015) Spring production of mycosporine-like amino acids and other UV-absorbing compounds in sea ice-associated algae communities in the Canadian Arctic. Mar Ecol-Prog Ser 541:91-104

Abstract:

Marine phytoplankton are known to produce mycosporine-like amino acids (MAAs) for protection against UV radiation. To assess whether the same strategy applies to sea ice-associated communities, MAAs were measured in algal communities associated with surface melt ponds, sea ice (bottom 3 cm), sea ice–water interface below melt ponds, and underlying seawater in a coastal bay of the Canadian Arctic Archipelago during the spring melt transition from snow- to melt pond-covered sea ice. Six UV-absorbing compounds (UVACs) were detected as the spring melt progressed, three of which are identified to be shinorine, palythine, and porphyra-334. A fourth UVAC (U1) is most likely palythene. The molecular identities of the other two UVACs, U2 and U3, which have an absorption maximum of 363 nm and 300 nm respectively, remain to be structurally elucidated. The greatest UVAC nominal concentrations were observed in the 3-cm bottom ice under thin snow-covered sites just prior to complete snowmelt. Normalization to chlorophyll *a* content revealed that the greatest contribution to UV absorption from biota was associated with melt ponds that are exposed to the highest light

intensity. These results confirm that Arctic sea ice-associated communities are capable of producing photoprotectants, and that spatial and temporal variations in MAA and other UVAC synthesis are affected by snow cover and UV radiation exposure.

2.1 Introduction

Ultraviolet (UV) radiation (280–400 nm) causes a reduction in photosynthetically incorporated carbon (Villafañe et al. 2004), although the extent of this photoinhibition is variable among species due to different protective strategies. One such strategy that many algae use to

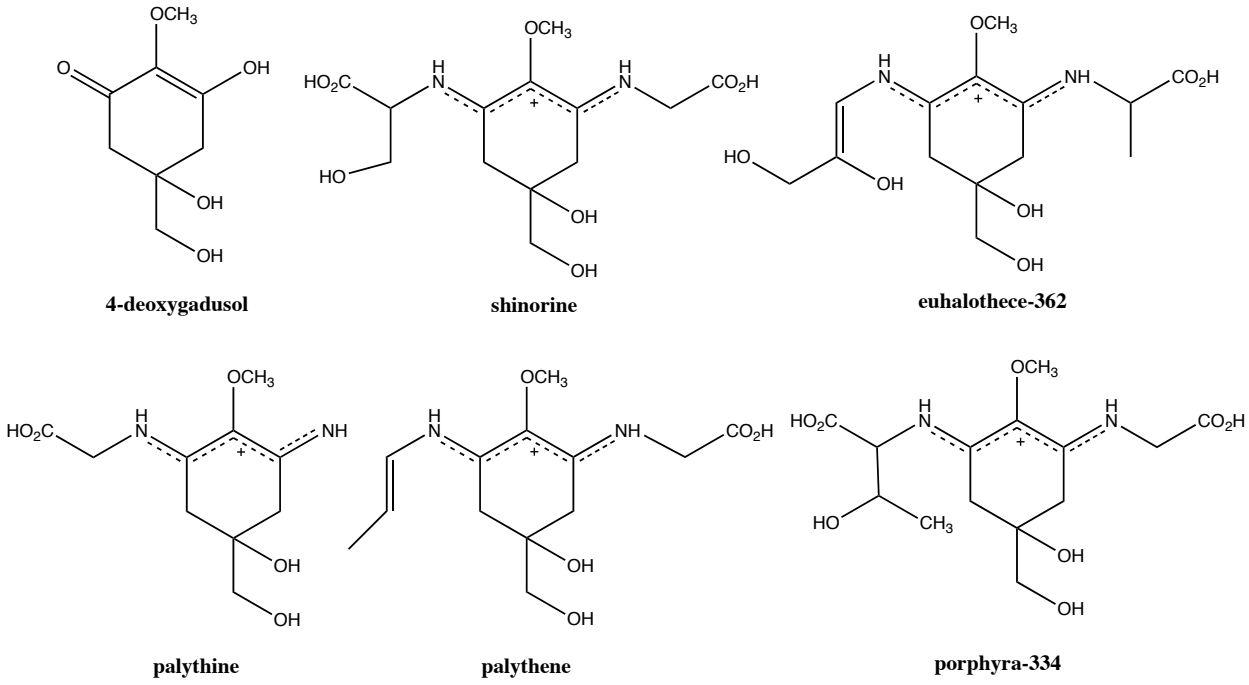

Figure 2.1 Structures of 4-deoxygadusol and a few example mycosporine-like amino acids referred to in this study.

protect against the detrimental effects of UV radiation is the production of mycosporine-like amino acids (MAAs), which are water soluble, UV-absorbing compounds of small molecular weight (Shick & Dunlap 2002). The precursor for this class of molecules is 4-deoxygadusol (Figure 2.1), the biosynthesis of which is presumably through the shikimate or pentose phosphate

pathway (Spence et al. 2012). The addition of amino acids, amino alcohols and other amino groups results in the formation of a variety of MAAs, over 20 of which have been structurally elucidated to date (Carreto & Carignan 2011) (a few example MAAs are shown in Figure 2.1). These compounds each have a characteristic absorption peak with a λ_{max} between 309–362 nm (Carreto et al. 2005, Carreto & Carignan 2011, Gao & Garcia-Pichel 2011). MAAs may also be involved in other cellular functions such as antioxidation (Dunlap & Yamamoto 1995, Suh et al. 2003), molecular repair (Shick & Dunlap 2002), and osmotic regulation (Oren 1997). In tropical and temperate oceans experiencing high UV radiation, the ability to synthesize or acquire MAAs appears to be primarily by pelagic dinoflagellates, diatoms, prymnesiophytes, macroalgae (most commonly red algae), and cyanobacteria (Karsten et al. 1998, Sinha et al. 2001, Sommaruga et al. 2009).

Algal communities in ice-covered polar seas inhabit environments that are characterized by strong gradients in solar radiation, temperature, and salinity. During spring melt, the sea ice surface transitions from cold dry snow cover to melt pond coverage. During this transition the amount of incident photosynthetically active radiation (PAR, 400–700 nm) transmitted through sea ice can exponentially increase over just a few weeks from <1% to 5–22% and 21–67% under white ice (i.e. drained surface ice above the local water table) and melt ponds, respectively (Ehn et al. 2011, Mundy et al. 2014). This transition coincides with the timing of peak downwelling irradiance resulting in exposure of sea ice and associated communities to high concentrations of UV radiation and PAR. Further, the effect can be further amplified by light scattering at the ice surface and within the sea ice. During the melt transition sea ice-associated algae living at the surface, within and immediately under the sea ice can potentially exhibit considerable photoprotective strategies including the production of MAAs. However, the occurrence and

temporal evolution of MAAs, and their relative importance in UV radiation attenuation in ice-associated communities remain poorly known. By exposing an Antarctic bottom ice algal community to UV radiation *in situ* for 15 days, Ryan et al. (2002) detected low concentrations of MAAs, and concluded that MAAs may only play a minor role as photoprotectants in sea ice algae. In contrast, relatively high MAA concentrations were measured in the surface layer of landfast ice in the Baltic Sea, upon the melting of snow (Uusikivi et al. 2010), in snow-covered ice and in snow-free ice upon experimental exposure to UV radiation (Piiparinen et al. 2015). The difference between these studies could be due to the exposure of the surface community to greater light intensity in the studies of Uusikivi et al. (2010) and Piiparinen et al. (2015), resulting in more high-light acclimated algae than that of the bottom ice community investigated in Ryan et al. (2002). MAAs were also measured in phytoplankton communities in spring near the ice edge along the Svalbard coast of the Arctic Ocean, though their concentrations were lower than those in open water away from the ice margin (Ha et al. 2012).

Rapid decreases in Arctic sea ice thickness and extent (Comiso et al. 2008) and an earlier melt onset (Maslanik et al. 2011) are causing light intensity to increase within and below the ice-covered Arctic Ocean during the spring season (Nicolaus et al. 2012). This changing light regime may also be influenced by winter- and spring-time decreases in stratospheric ozone over the Arctic (Rex et al. 1997, Manney et al. 2011). Therefore, the Arctic sea ice-associated biota is at a time of particular vulnerability to the increasing UV radiation. Studies on the capacity of primary producers in the Arctic to endure light stressor through the production of MAAs and other UV-absorbing compounds are thus an important step in our ability to predict and model ecosystem response to climate warming.

When studying the absorption spectra of algal samples taken from landfast first-year sea ice in a coastal Arctic bay, Mundy et al. (2011) noted that the wavelengths of peak UV absorption (310, 320–334, and 360 nm) corresponded to the absorption peaks of a variety of MAAs, with much higher absorbance observed in melt-pond algal samples than those within the sea ice. They also observed different UV wavelength peaks in different algal communities. Based on these results, we hypothesize that algae in different sea ice-associated environments will produce variable quantities and types of MAAs depending on their habitat exposure to light. We report here measurements of MAAs in Arctic algal communities associated with bottom ice, melt water, and water column habitats over the spring melt transition and in relation to changing environmental conditions. More specifically our study aimed to: (1) determine the presence or absence of MAAs in ice and ice-covered Arctic waters; (2) compare MAA composition in the different ice-associated habitats; (3) investigate the effect of snow cover on MAA production; and (4) relate the presence of specific MAAs to key algal taxa.

2.2 Materials and Methods

2.2.1 Study Area

Samples from the bottom ice, surface melt ponds, the sea ice–water interface below melt ponds, and the underlying seawater were collected from Allen Bay, Nunavut, Canada at an ice camp field site (74°43' N, 95°09' W) as part of the Arctic-ICE (Ice Covered Ecosystem) 2011 field program. The camp was located on smooth landfast first-year sea ice over a water depth of 60 m; details of the study site can be found elsewhere (Campbell et al. 2014, Galindo et al. 2014, Landy et al. 2014). The study period covered the transition from a snow-covered surface through to formation of melt ponds from 6 May to 24 June, 2011. Daily averaged air temperatures at the study site ranged from –16 to 4.1°C as the study progressed (Figure 2.2a). Site-averaged sea ice

thickness was near constant at 140 cm from the beginning of the study until 12 June, and decreased to 100 cm by 24 June (Galindo et al. 2014). Site-averaged snow depth varied between

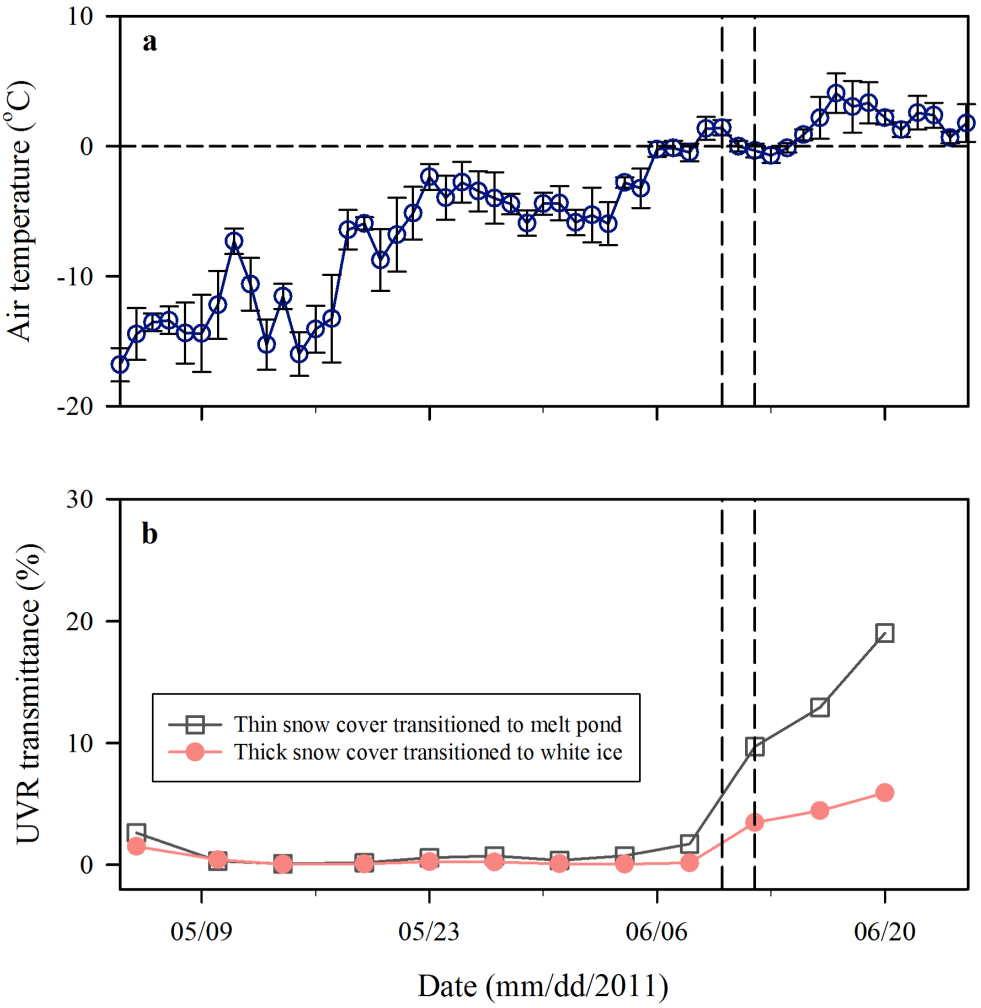

Figure 2.2 (a) Daily-average air temperature and (b) percent transmission of a narrow UV band (350–360 nm) through sea ice in Allen Bay, Nunavut, Canada between 6 May and 24 June, 2011. Percent transmission of a broader UV band (350–400 nm) followed the same trend. Dashed lines indicate two rainfall events on 10 and 12 June. In (a), error bars show the standard deviation.

15 and 20 cm before decreasing abruptly following rainfall events of 1.0 and 0.8 mm on 10 and 12 June, respectively, leading to the rapid development of melt ponds (Campbell et al. 2014). Sea ice break-up occurred on 27 June, shortly after termination of the study.

2.2.2 Sample Collection

Landfast sea ice core samples were taken every four days as part of a regular sampling schedule during the study period. All sampling occurred within an approximate 500 × 500 m area with new sampling sites chosen daily within a 50 m radius to include locations of thin (< 10 cm), medium (10–18 cm), and thick (>18 cm) snow depths. As the snow cover melted, the thin and thick snow sites transitioned to melt pond- and white ice-covered, respectively, and the medium snow sites were no longer sampled. Ice cores were collected by a Mark II Kovacs core barrel (i.d. = 9 cm) and the bottom 3 cm was used for ice algal samples. Two to three ice cores were pooled in isothermal cooler jugs and melted in the dark over 18−24 h with the addition of 0.2 µm-filtered seawater (FSW) at a volume ratio of approximately 3:1 (FSW:ice melt) to minimize osmotic shock of the microbial community and associated release of MAAs from cells while melting (Garrison & Buck 1986). An extra core (non FSW-diluted) at each site was also collected for bulk salinity measurement.

Sampling of the surface melt ponds and sea ice–water interface below melt ponds commenced on 12 June and occurred every four days to study their spatial and temporal variability. Spatial sampling involved selecting three to four melt ponds in the vicinity of the ice core collection site providing true replicates. Melt ponds were selected based on the criteria that no connection existed between them by surface drainage channels and that they had a depth of at least 3 cm. Slurp guns were used to collect surface melt pond samples. For collecting samples at the sea ice-water interface, auger holes were made through white ice adjacent to the melt pond, and the water samples were collected at the ice-water interface directly below the melt pond by a battery operated submersible pump (Cyclone®) positioned by an under-ice arm. The habitat sampled by this method will hereinafter be referred to as the interface below melt ponds. This

technique allowed us to sample the under-ice melt layer as it progressed to inverted melt ponds (Eicken et al. 2002).

Water column samples at 2, 5, and 10 m depths below the ice were collected every four days between 7 to 23 June using Niskin bottles deployed through a large ice hole within a heated tent (no replicates).

2.2.3 Sample Analysis

Salinity of water and non FSW-diluted melted sea ice core samples was measured with a handheld conductivity meter (Cond 330i, WTW). Downwelling irradiance (W m^{-2} nm^{-1}) was coincidentally measured at the surface and under the sea ice at each snow depth site using a dual head VIS-NIR spectrometer (350–1050 nm at 1.4 nm band width; FieldSpec Pro, Analytical Spectral Devices Inc.) with cosine corrected sensors and positioned using an under-ice arm (Campbell et al. 2014). Integrated percent transmittance (%T) over the MAA-relevant band of UV radiation (350–360 nm; data were not available for $\lambda < 350$ nm) was calculated using:

$$\%T = \frac{\int Ez_\lambda d\lambda}{\int Eo_\lambda d\lambda} \times 100\% \qquad (1)$$

where λ is wavelength and Ez_λ and Eo_λ are spectral transmitted and incident irradiance, respectively.

Water and melted FSW-diluted ice core samples were subsampled for determining protist taxonomy, concentrations of chlorophyll *a* (Chl *a*) and abundance of MAAs. Subsamples for identification and enumeration of diatoms, dinoflagellates and flagellates were preserved with acidic Lugol's solution (Parsons et al. 1984) and stored in the dark at 4°C until analysis. Cells ≥ 2 μm in size were identified to the lowest possible taxonomic rank (Poulin & Cardinal 1982a,b,1983, Medlin & Hasle 1990, Medlin & Priddle 1990, Thomsen 1992, Poulin 1993,

Tomas 1997, von Quillfeldt 1997) using an inverted microscope (Zeiss Axiovert 10) equipped with phase contrast optics (Lund et al. 1958). At least 400 cells were enumerated over a minimum of three transects. The abundance of each taxon was computed according to the equation described by Horner (2002).

Chl *a* was fluorometrically determined from 25–1000 ml of subsamples filtered onto a Whatman GF/F glass fiber filter (0.7 µm nominal pore size) using the methods of Parsons et al. (1984). Filters were immediately placed into 10 ml of 90% acetone and left at 4°C for 18−24 h in the dark for pigment extraction. Fluorescence of the extracted pigments was measured before and after acidification with 5% HCl using a 10-005R Turner Designs fluorometer. Chl *a* was calculated using the equation described by Holm-Hansen et al. (1965).

For MAA determination, 25–500 ml subsamples and daily field blanks (FSW) were filtered onto Whatman GF/F filters and stored at –80°C until analysis in the Manitoba Chemical Analysis Laboratory, Winnipeg, MB. The high performance liquid chromatography (HPLC) method used to quantify MAAs followed the procedure of Carreto et al. (2005). Briefly, field samples (filters containing particulate fractions of the water/melted ice samples) were taken from storage (−80°C freezer) and placed in a freezer at −20°C for 12−24 h prior to analysis. The samples were extracted via serial extraction with three aliquots of 2 ml of 100% methanol with the assistance of sonication in an ice bath. The 6 mL of solvent was then evaporated off with nitrogen and then reconstituted with 0.5 ml of the starting mobile phase (0.2% trifluoroacetic acid in water adjusted to pH = 3.15). Lab blanks and 200 mg of seaweed (*Porphyra* sp.) was extracted and run with each batch of samples as a quality control. Clean-up was done using ultracentrifugation filtration (Amicon 0.5 ml 100 kDa, Fisher Scientific) and the filtrates were analyzed within 24 h on a Varian Prostar HPLC with a diode array detector (DAD) at a flow rate

of 1 ml min^{-1}. The columns used were a C18 HL Alltima HP 150 mm × 4.6 mm × 5 μm (Fisher Scientific) in tandem with a C18 UG 120A 250 mm × 4.6 mm × 5 μm (JM Science). UV absorbance was monitored in the wavelength range of 280–400 nm with a particular focus on 360 and 330 nm to measure individual MAAs, as well as at 270 nm to monitor for interfering contaminants that absorb at lower wavelengths (Carreto et al. 2005). Due to the lack of MAA standards, the initial tentative identification of MAAs was simply based on comparing the values of retention time and λ_{max} with those reported in literature.

About one year after the initial HPLC-DAD analysis, we obtained three MAA standards (shinorine, palythine and porphyra-334, Figure 2.1) from Dr. A. Matsuoka of Université Laval (Quebec, Canada). This allowed us to carry out further identification of the MAAs in our samples on a HPLC (Agilent 1200)-eletrospray ionization (ESI)-triple quadrupole mass spectrometer (MS) (Agilent 6410b) in the Ultra-Clean Trace Elements Laboratory (UCTEL) at the University of Manitoba. The HPLC method was similar to the one described above, with the exception that trifluoroacetic acid in the mobile phase was replaced by formic acid to optimize ESI as suggested by Carignan et al. (2009). A multiple reaction monitoring (MRM) method was developed with ESI in positive mode (gas temperature = 325°C, gas flow = 11 l min^{-1}, and nebulizer pressure = 60 psi) based on the mixed solution of shinorine, palythine and porphyra-334. In brief, we first identified the major parent ion of each of the MAA standards (m/z = 333, 245, and 347 for shinorine, palythine and porphyra-334, respectively) under a fragmentor voltage of 100 V, and then monitored the major product ion (m/z = 230, 186, and 303 for shinorine, palythine and porphyra-334, respectively) at a collision energy of 20 eV. The MRM method was then used to confirm the identities of the MAAs in a sub-set of the previously analyzed samples. Upon obtaining the standards of three MAAs we compared concentrations estimated using molar

extinction coefficients and those derived from a calibration curve. We were unable to obtain consistent results therefore we prefer to express the MAA and other UVAC concentrations in the nominal unit of mAU l^{-1} (nominal concentration).

2.2.4 Statistical Analysis

Statistical analysis was performed with Prism (version 5.0a, GraphPad). Two-tailed Student's t-test was used to evaluate the difference between MAA nominal concentrations in various communities, and Pearson correlation was done to evaluate the relationship between taxonomic groups and MAAs. Significance threshold was set at $p < 0.05$.

2.3 Results

During the study period, daily-averaged air temperature steadily increased with some short-lasting, relatively stable periods (Figure 2.2a). The averaged temperatures first reached above 0°C on 9 June, and remained consistently near or above that value thereafter. High temperatures, along with two rainfall events on 10 and 12 June, resulted in rapid melting of snow, development of surface melt ponds and an under-ice melt layer, and thinning of sea ice (Campbell et al. 2014, Galindo et al. 2014). Percent transmittance of MAA-relevant UV radiation (350−360 nm) through snow and sea ice was < 1% until 4 and 8 June, respectively, and increased rapidly thereafter, reaching 19.0% and 5.9% by the end of the study under thin (melt pond) and thick (white ice) snow-covered sites, respectively (Figure 2.2b). The snow and then sea ice melt progression resulted in a slight increase in salinity in the surface melt ponds and a decrease in salinity of the 3-cm bottom ice, the interface below melt ponds, as well as the top 2 m of the underlying water column (Figure 2.3a-c).

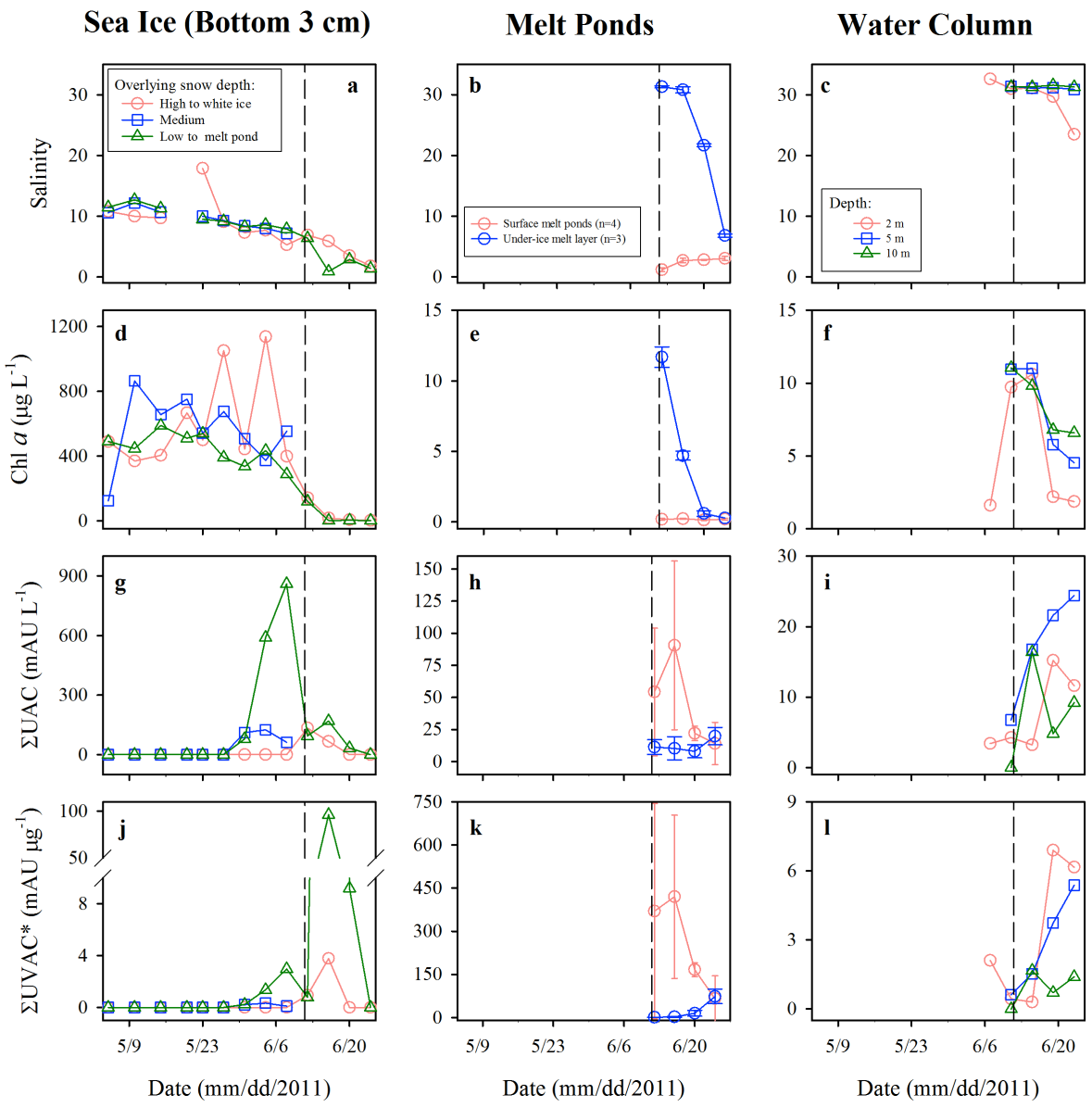

Figure 2.3 Time series of (a,b,c) salinity, (d,e,f) concentration of chlorophyll a (Chl a), (g,h,i) nominal concentration of total UV-absorbing compounds (∑UVAC), and (j,k,l) Chl a normalized ∑UVAC concentration (∑UVAC) in the 3-cm bottom ice (left panels), melt ponds (middle panels) and underlying water column (right panels) in Allen Bay, Nunavut, Canada between 6 May and 24 June, 2011. Dashed lines show when melt ponds started to develop following temperature rise and two rainfall events (June 12). In (b,e,h,k), error bars represent the standard deviation. UVAC concentrations include the three mycosporine-like amino acids (shinorine, palythine, porphyra-334) and three unknown UV-absorbing compounds (U1, U2, U3)*

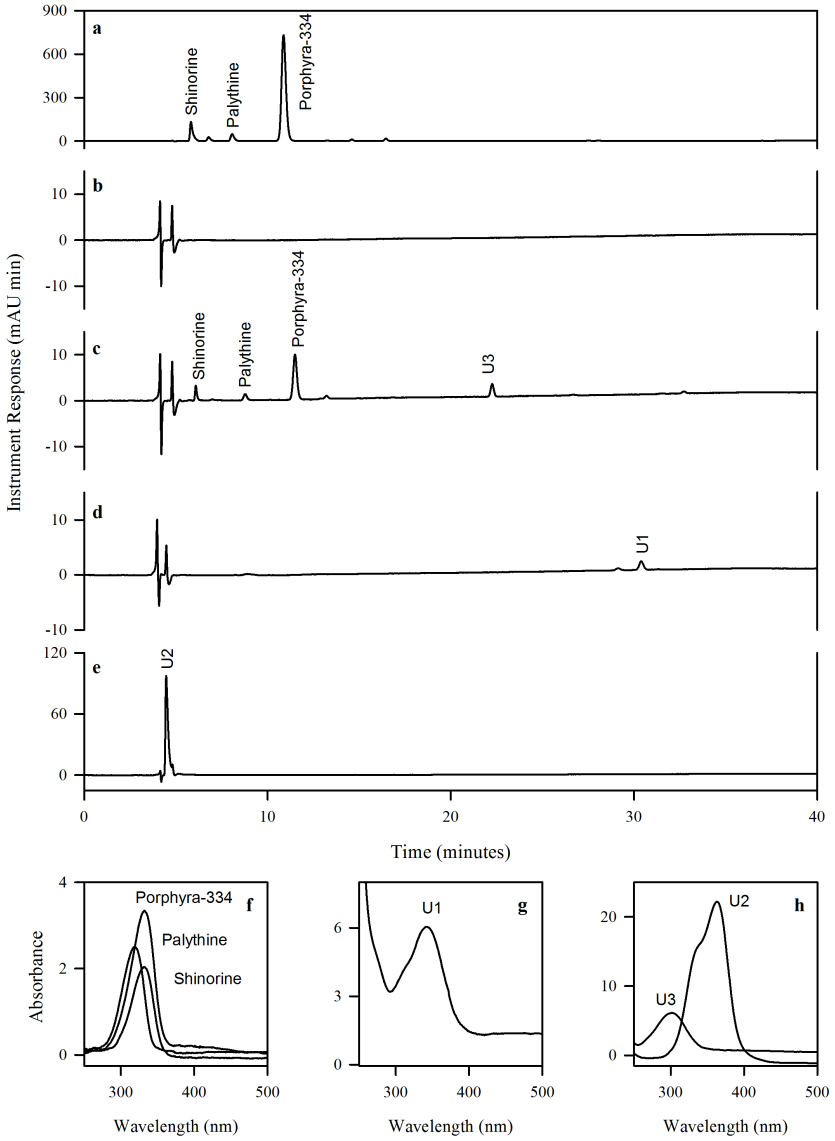

Figure 2.4 Chromatograms of (a) seaweed Porphyra sp. at 330 nm, (b) field blank (filtered seawater procedural blank) at 330 nm, (c) water column sample at 330 nm, (d) under-ice melt layer sample at 360 nm, and (e) surface melt pond sample at 360 nm. Bottom panels (f,g,h) show UV-visible absorption spectra of three mycosporine-like amino acids (shinorine, palythine, porphyra-334) and three unknown UV-absorbing compounds (U1, U2, U3)

Bottom ice Chl *a* concentrations varied between 400 and 1000 μg l^{-1} from 6 May to 4 June, then sharply decreased to <10 μg l^{-1} after 16 June (Figure 2.3d). Chl *a* concentrations in the surface melt ponds were consistently < 0.5 μg l^{-1} (Figure 2.3e). The interface below melt ponds had a much higher Chl *a* concentration (11.7 μg l^{-1}) on 12 June at the beginning of melt pond development, but decreased rapidly to < 0.5 μg l^{-1} by 20 June (Figure 2.3e). In the underlying water column, Chl *a* concentrations were < 0.5 μg l^{-1} at the beginning of the sampling period (Galindo et al. 2014), increased to a maximum of 11 μg l^{-1} on 11 June, and decreased thereafter (Figure 2.3f). A subsurface chlorophyll maximum began to form at a depth of 5−10 m at the end of the sampling period (Galindo et al. 2014).

For the analysis of MAAs, various peaks were present in the HPLC chromatograms of bottom ice samples collected after 31 May, and in most of the melt pond and water column samples collected. In total, six peaks were most consistently identified from HPLC chromatograms (*see* Figure 2.4c–e for examples). Their absorption maxima (λ_{max}) ranged from 300 to 363 nm (Figure 2.4f–h), which fell within the general range of those reported for MAAs (309–362 nm) with the exception of U3 (λ_{max} = 300 nm). Based on the comparison of retention times and λ_{max} with those reported in Carreto et al. (2005) and on the calibration with the seaweed *Porphyra* sp. (Figure 2.4a), four peaks were tentatively assigned to shinorine (λ_{max} = 332 nm), palythine (λ_{max} = 320 nm), porphyra-334 (λ_{max} = 333 nm), and palythene (λ_{max} = 358 nm). The identities of shinorine, palythine and porphyra-334 were later confirmed by HPLC-ESI-MS by monitoring the major mass transition of the corresponding standards (m/z 333→230 for shinorine, 245→186 for palythine, and 347→303 for porphyra-334) in a sub-set of the samples. Although the fourth compound (λ_{max} = 358 nm) is most likely palythene, we were not able to structurally confirm it due to the lack of an appropriate standard and due to the small

quantity of the samples; it will be referred to a UV-absorbing compound Unknown 1 (U1). The retention time and absorption spectrum of the remaining two peaks could not be matched to any of the 20 MAAs reported in Carreto et al. (2005), and hereafter are referred to as UV-absorbing compounds Unknown 2 (U2; retention time = 4.1 min, λ_{max} = 363 nm with a second λ_{max} = 337 nm) and Unknown 3 (U3; retention time = 19 min, λ_{max} = 300 nm). Structural identification of U2 and U3 by HPLC ESI-MS was not successfully due to the small quantity of our samples. Due to the lack of respective standards for calibration at the time of the analysis, accurate quantification was not possible and therefore the concentrations of shinorine, palythine,

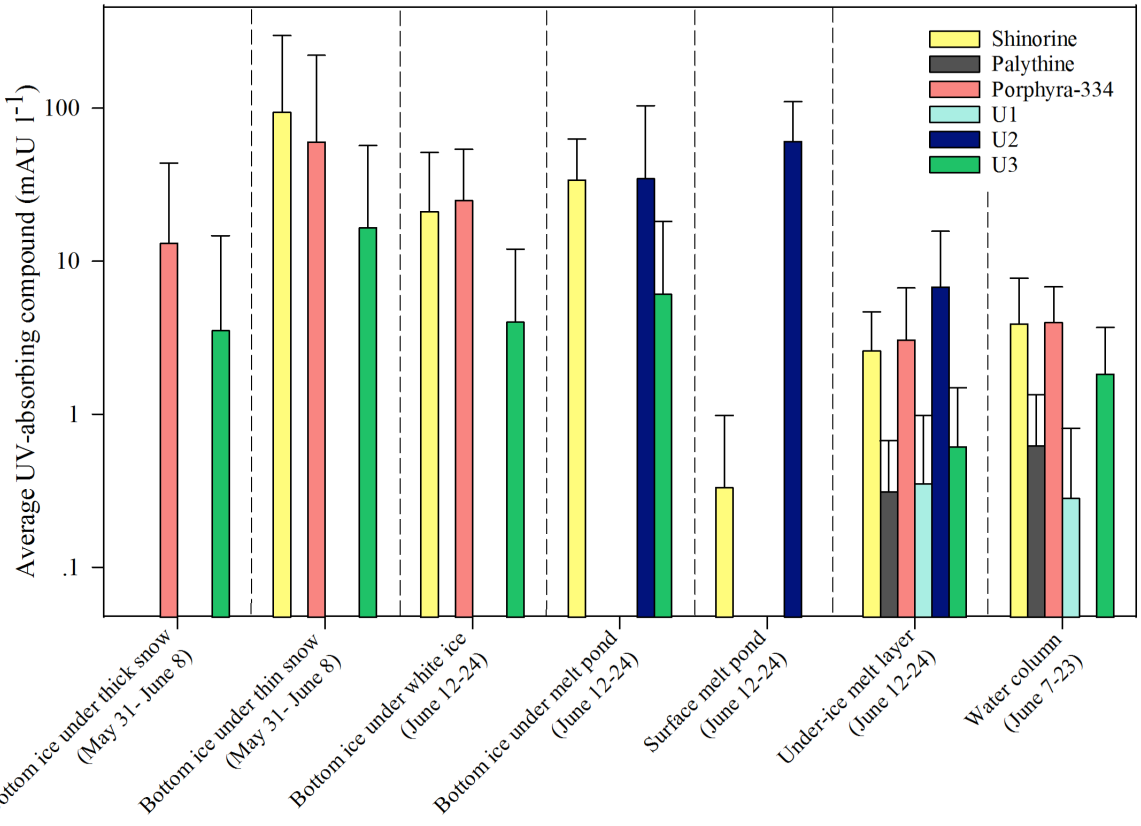

Figure 2.5 Average UV-absorbing compound concentrations from samples collected from different habitats in Allen Bay, Nunavut, Canada between 31 May and 24 June, 2011. Error bars represent the standard deviation.

porphyra-334, U1, U2, and U3 are reported nominally as their UV absorption capacity measured in mAU l^{-1} (milli absorbance units per liter of water or melted ice). The nominal concentration of total UV-absorbing compounds (UVAC), ∑UVAC, was calculated as the sum of shinorine, palythine, porphyra-334, and U1 – 3. As all the UVAC measurements were made on particles retained on filters, the concentrations reported herein refer to those in the particulate phase (i.e. within cells), not in the dissolved phase.

In the bottom ice, no UVACs were detected prior to 31 May at both thin and mid snow-covered sites. UVACs increased rapidly afterwards, reaching a peak ∑UVAC value of 860 mAU l^{-1} on 8 June at thin snow-covered sites and 125 mAU l^{-1} on 31 May at mid snow-covered sites (Figure 2.3g). At thick snow-covered sites, UVACs were not detected in the bottom ice horizon until 12 June with a ∑UVAC value of 133 mAU l^{-1} (Figure 2.3g). At all sites UVAC nominal concentrations in the bottom ice decreased quickly following the development of melt ponds and became undetectable by 24 June. ∑UVAC nominal concentrations in the surface melt ponds were between 65 and 90 mAU l^{-1} following the melt pond development at the surface of the ice, but decreased rapidly to ~10 mAU l^{-1} as melting and drainage progressed (Figure 2.3h). In contrast, ∑UVAC nominal concentrations in the interface water below the melt ponds were initially below 15 mAU l^{-1} and increased as drainage of the surface melt ponds progressed (Figure 2.3h). By the end of the study ∑UVAC nominal concentrations in the interface water below the melt ponds were not different from those in the surface melt ponds ($p = 0.90$, $n = 3$, t-test). In the underlying water column ∑UVAC nominal concentrations ranged from below the detection limit to 24 mAU l^{-1}, with concentrations generally higher at 5-m depth than at the 2- and 10-m depths (Figure 2.3i).

In order to examine the relative production of UVACs per algal biomass, Chl *a*-specific ∑UVAC were calculated (∑UVAC*; mAU μg^{-1} Chl *a*). Although the bottom ice under thin snow cover had the highest ∑UVAC nominal concentrations, surface melt pond algae had the highest ∑UVAC*, 420 mAU μg^{-1} (Figure 2.3k). Comparable ∑UVAC* were found in the bottom ice algae (up to 96 mAU μg^{-1}) and in the interface water under melt ponds (Figure 2.3j,k). Much lower ∑UVAC* were observed in the water column (2–10 m water depths; up to 6.9 mAU μg^{-1}), and in the bottom ice under white ice (up to 3.8 mAU μg^{-1}). Bottom ice under medium to thick snow cover had the lowest ∑UVAC* (<0.5 mAU μg^{-1}; Figure 2.3j).

In terms of UVAC composition, the most abundant MAAs in all the samples were shinorine and porphyra-334 (Figure 2.5). The unknown UV-absorbing compound, U2, while present in the bottom ice under melt pond and in the under-ice melt layer, contributed greatly in surface melt ponds. U2 had the highest Chl *a*-specific nominal concentration of UV-absorbing compounds observed (88–560 mAU μg^{-1}), followed by shinorine, and then by other MAAs and

Table 2.1 Pearson's correlation coefficients of shinorine, palythine, porphyra-334, and three unknown UV-absorbing compounds (U1, U2 and U3) with total flagellate and flagellate group abundance in the water column samples from Allen Bay, Nunavut, Canada. Only those that are significant at $p < 0.05$ are shown.

Group	Taxon	Shinorine	Palythine	Porphyra-334	U1	U2	U3
Prasinophytes	*Pyramimonas* spp. (6–10 µm)		0.79	0.83			
	Pyramimonas cf. *nansenii* Braarud		0.76				
	Total	0.77		0.79			
Prymnesiophytes	*Chrysochromulina* spp. (2–5 µm)	0.79		0.81			
	Chrysochromulina spp. (6–10 µm)			0.76			
	Prymnesiophyceae spp. (2–5 µm)						–0.86
	Total			0.81			
Total flagellates				0.84			

U3 with relatively minor Chl *a*-specific nominal concentrations. The diversity of UVAC composition was the highest in the under-ice melt layer and lowest in surface melt ponds. In samples collected for taxonomic analyses, the total abundance of protists (i.e. sum of diatoms, dinoflagellates and flagellates) was, on average, 0.29×10^6 cells l^{-1} in surface melt ponds (June), 114×10^6 cells l^{-1} in bottom ice under thick snow cover (May and June) and 5.38×10^6 cells l^{-1} and 4.53×10^6 cells l^{-1} in the water column at 5 m and 10 m depth, respectively (June). The surface melt pond protist community was numerically dominated by flagellates (75%) among which a large proportion (88%) was unidentified taxa. The rest of the community was composed of pennate (16%) and centric diatoms (7%), and dinoflagellates (2%) (Figure 2.6a). The bottom ice community was dominated by pennate diatoms (72%) with the pan- Arctic endemic species,

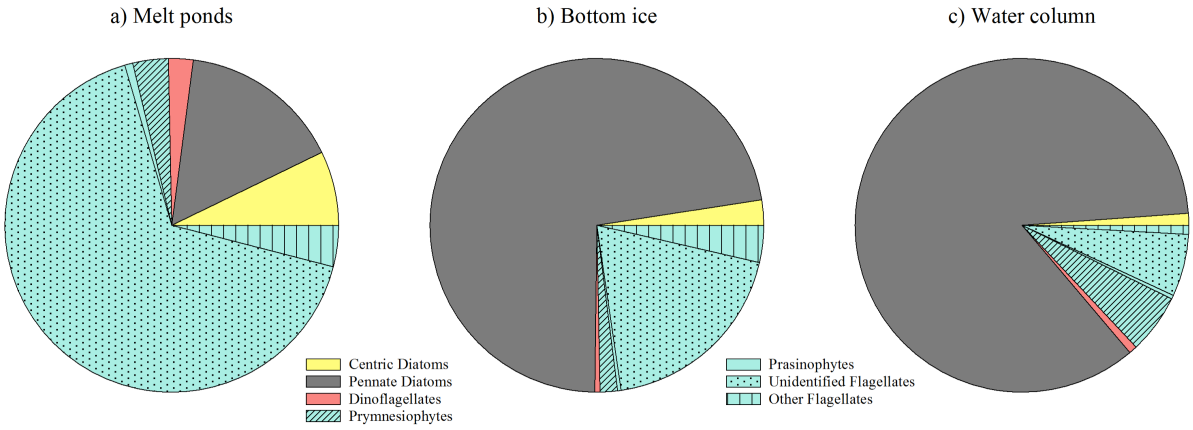

Figure 2.6 Average relative abundance of 6 protist (> 2 µm) groups (centric diatoms, pennate diatoms, dinoflagellates, prymnesiophytes, prasinophytes, unidentified flagellates and other flagellates) in (a) melt ponds (June), (b) bottom ice (bottom 3 cm of sea ice) under a thick snow cover (>15 cm, May and June), and c) water column (5 m depth, June) in Allen Bay, Nunavut, Canada. The other flagellate group comprises chlorophytes, chrysophytes, cryptophytes, dictyochophytes, euglenophytes and raphidophytes. Note that we did not observe dictyochophytes in melt pond samples and chrysophytes, dictyochophytes and raphidophytes in bottom ice samples.

Nitzschia frigida Grunow, making up 14–46% of the total cell abundance. Other protist groups present in the bottom ice horizon were flagellates (25%), centric diatoms (2.5%) and

dinoflagellates (0.5%) (Figure 2.6b). As in the bottom ice, pennate diatoms were predominant in the water column community at 5 m (85%) (Figure 2.6c), but *Fossula arctica* Hasle, Syvertsen & von Quillfeldt was the main species representing 42−76% of the total cell abundance. The rest of the community was composed of flagellates (13%), centric diatoms (1.2%), and dinoflagellates (0.8%) (Figure 2.6c).

2.4 Discussion

2.4.1 Identity of MAAs in Ice-Covered Environments

The three MAAs, shinorine, palythine and porphyra-334, identified in the ice-covered water column and under-ice melt layer in this study, have all been previously reported in polar waters (Karentz et al. 1991, Whitehead et al. 2001, Ryan et al. 2002, Ha et al. 2012). Of particular relevance to this study in the Arctic Ocean is Ha et al. (2012), which detected five MAAs in phytoplankton samples collected near Svalbard, namely shinorine, palythine, porphyra-334, asterina-330 and mycosporine-glycine. In contrast, there was no conclusive evidence of asterina-330 and mycosporine-glycine in any of our samples. Another UVAC, U1 (most likely palythene), was found to be present in our water column and under-water melt layer samples, but was not reported in Ha et al. (2012). Similarly, while shinorine, palythine and porphyra-334 were detected in the sea ice of the Baltic Sea (Uusikivi et al. 2010, Piiparinen et al. 2015), only shinorine and porphyra-334 were identified in our bottom sea ice samples. Such difference could be due to the presence of different organisms in different regions. For example, *Phaeocystis* sp. was a dominant phytoplankton species observed in Ha et al. (2012), whereas our water column samples were dominated by pennate diatoms (mainly *F. arctica*) with *Phaeocystis* sp. only present at very low abundances (3% of total flagellates and 0.3% of total protist cells). Palythine was detected in Baltic Sea ice that was thinner (33–40 cm) than the ice sampled in our study

(100–140 cm). In sea ice, shorter wavelength radiation in the UV spectrum is attenuated more rapidly than longer wavelengths. It is possible that in the case of our samples the bottom ice algae had less need for palythine, which has an absorption maximum at a shorter wavelength (320 nm).

The two other unknown UV-absorbing compounds U2 (λ_{max} = 363 nm) and U3 (λ_{max} = 300 nm) absorbed light at the extreme end and outside, respectively, of the λ_{max} range of the known MAAs. U2 also had a shoulder in the absorption curve centered at 337 nm (Figure 2.3h), similar to an unknown compound recently reported in the Baltic Sea ice upon exposure to high UV radiation (Piiparinen et al. 2015). Piiparinen et al. (2015) speculated the identity of this unknown to be M335/360, a condensation product of shinorine and palythene as reported in Carreto et al. (2001). However, the absorption spectrum and chromatographic retention for M335/360 does not match that of U2. While M335/360 has a large peak at 335 nm and a shoulder at 360 nm, U2 had a large peak at 363 nm and a shoulder at 337 nm. Although the different HPLC methods used in our study and in Carreto et al. (2001) do not allow for a direct comparison of retention times, it is important to note that M335/360 eluted off their column (Alltima Alltech C18) after shinorine, whereas U2 was the first to elute off our columns. This suggests U2 is more polar than M335/360. The only known MAAs that have an absorption maximum close to 360 nm are usujirene (λ_{max} = 357 nm), palythene (λ_{max} = 360 nm), and euhalothece-362 (λ_{max} = 362 nm). It is possible that U2 could be a condensation product of one of these compounds and another MAA, although the large difference in retention times between U2 and palythene or usujirene in our analysis suggests that neither palythene nor usujirene can be a component of U2. Euhalothece-362 is also only weakly acidic and has higher retention to C8 bonded silica than strongly acidic MAAs such as shinorine, porphyra-334 and mycosporine-

2-glycine (Volkmann et al. 2006). U2 demonstrates similar retention properties as strongly acidic MAAs; from this observation we propose that U2 cannot be euhalothece-362 although it may be a condensation product of this compound and a strongly acidic MAA. To date, euhalothece-362 has only been identified in the halophilic cyanobacterium, *Euhalothece* sp. (Oren 1997, Volkmann et al. 2006), but it is suspected to be more widespread in unicellular cyanobacteria (Volkmann et al. 2006). While our understanding of MAAs in marine cyanobacteria is poor, the possibility of MAA association with symbiotic cyanobacteria contained within heterotrophic dinoflagellates or diatoms has been reported from a study along a surface water meridional transect of the Atlantic Ocean (Llewellyn et al., 2012). Cyanobacteria have recently been observed in Arctic marine habitats including seawater (Bowman et al. 2012, Diez et al. 2012), first-year (Mundy et al. 2011) and multi-year sea ice (Bowman et al. 2012), and sea ice brine (Diez et al. 2012). No filamentous cyanobacteria of ≥ 2 μm in size were observed by inverted microscopy in any of our samples. Although we did not enumerate picocyanobacteria cells (< 2 μm) during this study, we did find a very small number of picocyanobacteria, by flow cytometry, in melt ponds, bottom ice and water column from the same site a subsequent study in late June 2012. Future structural identification is needed to determine if U2 is a condensation product of euhalothece-362 and another MAA, a novel, previously unreported MAA, or a non-MAA UV-absorbing compound.

U3 had an unusually short λ_{max} of 300 nm. In comparison, the MAA "backbone" 4-deoxygadusol has a λ_{max} of 268 nm, and mycosporine-glycine, which is among the least conjugated MAA, has a λ_{max} of 310 nm (Carreto et al. 2005, Gao & Garcia-Pichel 2011). We suggest it might be structurally impossible to have an MAA with a λ_{max} of 300 nm and therefore, U3 is likely a novel, non-MAA, UV-absorbing compound that requires structural elucidation.

2.4.2 Estimate Concentrations of MAAs

Since we did not obtain the MAA standards until one year after the analysis was done, we were not able to directly determine concentrations. To compare with the literature data, we estimated the concentrations of the three MAAs from the absorbance, the pathlength of the flow cell (1 cm), the published molar extinction coefficient and the molecular weight of 44700 l mol^{-1} cm^{-1} and 332 g mol^{-1} for shinorine, 36200 l mol^{-1} cm^{-1} and 244 g mol^{-1} for palythine, and 42300 l mol^{-1} cm^{-1} and 346 g mol^{-1} for porphyra-334 (Gröniger et al. 2000, Carreto et al 2011). The estimated concentrations of shinorine ranged between 0.1 – 21.9 μg l^{-1} and were greatest in the bottom sea ice beneath a low snow cover. Palythine estimated concentrations did not exceed 0.1 μg l^{-1} throughout the study and trace levels were seen in the water column at all depths sampled. Estimated concentrations of porphyra-334 were between 0.1 – 19.9 μg l^{-1}. Assuming U1 is palythene with a molar extinction coefficient of 50000 l mol^{-1} cm^{-1} (Gröniger et al. 2000, Carreto et al 2011), its concentrations estimated remain at trace levels (<0.1 μg l^{-1}) throughout the study and were confined to the water column. These values are in a similar range as those estimated in Baltic Sea ice (1.1 – 2.5 μg l^{-1} total MAAs in bottom sea ice) (Piiparinen et al. 2015) as well as those measured in the Arctic waters near Svalbard (3.1 – 25.5 μg l^{-1} in water column) (Ha et al. 2012). If we compare the ratio of the total estimated MAA concentrations to Chl *a* concentrations (μg l^{-1}), the ratios in our bottom ice samples are up to 0.6, which is much greater than those reported in Baltic sea ice (0.008 ± 0.004) (Piiparinen et al. 2015). The high ratios that we have observed are during the late stages of sea ice melt and this seasonal transition was not captured in the work of Piiparinen et al. (2015). Cautions are warranted when estimating MAA concentrations based on their molar extinction coefficients, as the coefficients are known to vary with analytical conditions (e.g. pH, temperature) (Zhang et al. 2005). For instance, our samples

are measured at a pH of 2.2 – 3.15, which may affect our estimates as well as others who use this method of quantification.

2.4.3 Origins of MAAs in Different Ice-Covered Environments

Shinorine, porphyra-334 and U3 were present consistently throughout the water column and within most of the ice algae communities sampled (Figure 2.5), suggesting their production within both environments. Porphyra-334 has been identified previously as the dominant MAA present in Antarctic ice algae communities (Karentz et al. 1991, Ryan et al. 2002), consistent with our samples collected under thick and medium snow cover. In contrast, samples collected beneath thin snow covers, and eventually melt ponds, contained shinorine as the dominant identified MAA. This observation suggests that shinorine production may be preferred for ice algae under greater light stress. Palythine and U3 were only detected in the water column and interface water under melt ponds, suggesting production was associated mainly with the water column environment (Figure 2.5).

Of potential significance is that the structurally unidentified U2 was only observed in samples associated with melt ponds (e.g. surface melt ponds and bottom ice and interface water below melt ponds). It is important to note that U2 was never detected in bottom ice algae under snow- (i.e. prior to melt pond development) and white ice-cover, and in the water column underneath the ice at 2, 5, and 10 m depths. These observations suggest that U2 is uniquely associated with sea ice melt upon its exposure to greater UV radiation, which would agree well with its presence in the Baltic Sea ice upon experimental exposure to UV (Piiparinen et al. 2015). It can also be noted that U2 was only present when Chl *a* concentrations were very low and light exposure was high. This suggests that it may be produced during times of high light stress, when organisms are attempting to acclimate or survive.

2.4.4 Influence of light on production of UV absorbing compounds

The development of melt ponds leads to greater transmission of UV radiation into and through the ice cover. Through direct exposure to incoming solar radiation and enhanced back scatter associated with the high albedo of surrounding sea ice, surface melt ponds are exposed to the highest light intensity (Figure 2.2b; Perovich 2006, Ehn et al. 2011, Nicolaus et al. 2012). Few MAAs were encountered in melt ponds but the occurrence of U2 presents the possibility of alternate screening compound(s). A comparison of MAA production in the bottom ice under thick and thin snow covers demonstrated a greater abundance and earlier presence of MAAs under the thin snow cover (Figure 2.3d,g) where UV transmission (350–360 nm) increased first and more rapidly after 4 June (Figure 2.2b). This period corresponded to a rapid transition of thin snow to melt pond coverage, whereas the thick snow sites transitioned into a white ice cover. The ice-covered water column exhibited the lowest MAA nominal concentrations, which is to be expected, as it would have received the lowest irradiance.

The highest nominal concentrations of MAAs within the bottom ice were observed immediately prior to melt pond formation and the termination of the bottom ice algal bloom when ice Chl *a* concentrations were still high (Figure 2.3g,d). Termination of the bloom was influenced by warming of the ice cover, increased transmitted irradiance, and most notably rain events that caused sloughing off of the bottom ice protist community into the seawater (Campbell et al. 2014). It follows that the observed increase in MAAs was likely triggered by the higher UV transmission through the ice.

Bottom ice and interface water below melt ponds showed very high Chl *a*-specific UV absorbing compound nominal concentrations in comparison to both the bottom ice prior to melt pond development and the water column throughout the study period (Figure 2.3j-l). Surface

melt ponds, where UV transmittance is the greatest, contained organisms with a higher capacity to absorb UV light relative to Chl *a* concentrations. Chl *a* concentrations are likely reduced in melt pond organisms due to photoacclimation strategies in these high light regions, further contributing to high MAA:Chl *a* ratios. The high UV-absorption capacity of organisms in surface melt ponds not only offers direct UV protection to melt pond organisms, but may also contribute a layer of protection for underlying communities, reducing their need to produce these UV-absorbing compounds themselves.

2.4.5 Taxonomic Relationships

A linear correlation analysis was performed between UVAC nominal concentrations and protist group abundances using data collected in June. The only UVAC that was present within more than one of the analyzed melt pond samples ($n = 4$) was U2 and there was no significant correlation ($p > 0.05$) observed with any of the taxonomic protist groups identified (i.e. pennate diatoms, centric diatoms, flagellates and dinoflagellates). Within the water column samples analyzed ($n = 7$), MAAs were not significantly correlated with the most prominent water column species, the pennate diatom *F. arctica*. A significant ($p < 0.05$) positive correlation was only observed between MAA nominal concentration and the flagellate group. Therefore, we analyzed different flagellate taxa in water column samples (Table 2.1) and found a significant positive correlation between the total prasinophyte abundance with both shinorine ($r = 0.77$) and porphyra-334 ($r = 0.79$), of which its most prominent taxa, *Pyramimonas* spp. of 6–10 μm in size, had a significant positive correlation with palythine ($r = 0.79$) and porphyra-334 ($r = 0.83$). Furthermore, the total prymnesiophyte abundance showed a positive correlation with porphyra-334 ($r = 0.81$). The most dominant prymnesiophyte taxa, *Chrysochromulina* spp. of 2–5 μm in size, also demonstrated significant correlations with shinorine ($r = 0.79$) and porphyra-334

(r = 0.81). Finally, the Prymnesiophyceae (2–5 μm in size) showed a negative correlation with U3 (r = –0.86).

MAA production by the prymnesiophyte *Phaeocystis pouchetii* (Hariot) Lagerheim has been documented in Antarctic polar waters (Marchant et al. 1991) and in the Arctic near Svalbard (Ha et al. 2012); however, no significant correlation was seen between MAAs and *P. pouchetii* in this study. The significant correlations of *Chrysochromulina* spp. and *Pyramimonas* spp. with specific UVACs provide evidence that these species could be producing the compounds (Table 2.1). Indeed, Mundy et al. (2011) observed a dominance of prymnesiophytes and prasinophytes in melt water samples as well as strong UV-particulate absorption properties that inferred the production of MAAs. However, we caution that experimental studies need to be performed with cultures to determine if these taxa are in fact MAA-producing algae. It is possible that the absorption peak observed in the melt water samples by Mundy et al. (2011) was not palythene as speculated therein since this MAA was not observed within the melt ponds throughout this study. The presence of U2 is the likely absorbing constituent (similar λ_{max} observed around 360 nm and absorption shoulder near 334 nm, Mundy et al. 2011), although we are unable to confirm it at this time.

These results confirm that Arctic sea ice-associated communities are capable of producing MAAs and other UVACs, which may play an important role in the Arctic marine ecosystem's response to changing light regimes from a warming climate and/or changing stratospheric ozone concentrations. Further studies are warranted to structurally identify the unknown UV-absorbing compounds (U1, U2, U3), and to uncover the role of MAAs and other photoprotectants in the Arctic marine ecosystem as a whole.

2.5 Acknowledgements

This research was funded by Natural Sciences and Engineering Research Council (NSERC) of Canada, ArcticNet (Network of Centres of Excellence of Canada), Canada Economic Development, the Northern Scientific Training Program of the Aboriginal Affairs and Northern Development Canada, Fonds de recherche du Québec - Nature et Technologies (FRQNT), the Canadian Museum of Nature, and the University of Manitoba. The Arctic-ICE camp was logistically supported by the Polar Continental Shelf Program (PCSP) of Natural Resources Canada. We thank Virginie Galindo and Robin Bénard for their assistance in the field, Sylvie Lessard for the enumeration and identification of protists, Tim Papakyriakou for providing air temperature data, and Marjolaine Blais for the logistics. We are indebted to Dr. A. Matsuoka of Université Laval for providing shinorine, palythine and porphyra-334 standards to facilitate the structural identification. We thank three anonymous reviewers for their thorough and insightful comments on an earlier version of the manuscript. This is a contribution to the research programs of ArcticNet, Arctic Science Partnership (ASP), and the Canada Excellence Research Chair (CERC) unit at the University of Manitoba.

Literature Cited

Bowman JS, Rasmussen S, Blom N, Deming JW, Rysgaard S, Sicheritz-Ponten T (2012) Microbial community structure of Arctic multiyear sea ice and surface seawater by 454 sequencing of the 16S RNA gene. ISME J 6:11–20

Campbell K, Mundy CJ, Barber DG, Gosselin M (2014) Remote estimates of ice algae biomass and their response to environmental conditions during spring melt. Arctic 67: 375–387

Carignan MO, Cardozo KHM, Oliveira-Silva D, Colepicolo P, Carreto JI (2009) Palythine-threonine, a major novel mycosporine-like amino acid (MAA) isolated from the hermatypic coral *Pocillopora capitata.* J Photoch Photobio B 94:191–200

Carreto JI, Carignan MO (2011) Mycosporine-like amino acids: Relevant secondary metabolites. Chemical and ecological aspects. Mar Drugs 9:387–446

Carreto JI, Carignan MO, Montoya NG (2001) Comparative studies on mycosporine-like amino acids, paralytic shellfish toxins and pigment profiles of the toxic dinoflagellates *Alexandrium tamarense*, *A. catenella* and *A. minutum*. Mar Ecol Prog Ser 223:49–60

Carreto JI, Carignan MO, Montoya NG (2005) A high-resolution reverse-phase liquid chromatography method for the analysis of mycosporine-like amino acids (MAAs) in marine organisms. Mar Biol 146:237–252

Carreto JI, Roy S, Whitehead K, Llewellyn CA, Carignan MO (2011) UV-absorbing 'pigments': mycosporine-like amino acids. In: Roy S, Llewellyn CA, Egeland ES, Johnsen G (eds) Phytoplankton pigments: Characterisation, chemotaxonomy and applications in oceanography. Cambridge University Press, Cambridge, p 412–441

Comiso JC, Parkinson CL, Gersten R, Stock L (2008) Accelerated decline in the Arctic sea ice cover. Geophys Res Lett 35:L01703, doi:01710.01029/02007GL031972

Diez B, Bergman B, Pedros-Alio C, Anto M, Snoeijs P (2012) High cyanobacterial nifH gene diversity in Arctic seawater and sea ice brine. Environ Microbiol Rep 4:360–366

Dunlap WC, Yamamoto Y (1995) Small-molecule antioxidants in marine organisms: Antioxidant activity of mycosporine-glycine. Comp Biochem Physiol B: Biochem Mol Biol 112:105–114

Ehn JK, Mundy CJ, Barber DG, Hop H, Rossnagel A, Stewart J (2011) Impact of horizontal spreading on light propagation in melt pond covered seasonal sea ice in the Canadian Arctic. J Geophys Res Oceans 116:C00G02, doi:10.1029/2010JC006908

Eicken H, Krouse HR, Kadko D, Perovich DK (2002) Tracer studies of pathways and rates of meltwater transport through Arctic summer sea ice. J Geophys Res 107(C10):8046, doi:10.1029/2000JC000583

Galindo V, Levasseur M, Mundy CJ, Gosselin M, Tremblay J-É, Scarratt M, Gratton Y, Papakiriakou T, Poulin M, Lizotte M (2014) Biological and physical processes influencing sea ice, under-ice algae, and dimethylsulfoniopropionate during spring in the Canadian Arctic Archipelago. J Geophys Res 119:3746–3766, doi:3710.1002/2013JC009497

Gao Q, Garcia-Pichel F (2011) Microbial ultraviolet sunscreens. Nature Rev Microbiol 9:791–802

Garrison DL, Buck KR (1986) Organism losses during ice melting: A serious bias in sea ice community studies. Polar Biol 6:237–239

Gröniger A, Sinha RP, Klish M, Häder D-P (2000) Photoprotective compounds in cyanobacteria, phytoplankton and macroalgae – a database. J Photochem Photobiol B: Biol 58:115-122

Ha S-Y, Kim Y-N, Park M-O, Kang S-H, Kim H-C, Shin K-H (2012) Production of mycosporine-like amino acids of in situ phytoplankton community in Kongsfjorden, Svalbard, Arctic. J Photochem Photobiol Biol 114:1–14
Holm-Hansen O, Lorenzen CJ, Holmes RW, Strickland JDH (1965) Fluorometric determination of chlorophyll. J Cons Int Explor Mer 30:3–15
Horner RA (2002) A taxonomic guide to some common marine phytoplankton. Biopress Limited, Bristol
Karentz D, McEuen FS, Land MC, Dunlap WC (1991) Survey of mycosporine-like amino-acid compounds in Antarctic marine organisms – potential protection from ultraviolet exposure. Mar Biol 108:157–166
Karsten U, Sawall T, Hanelt D, Bischof K, Figueroa FL, Flores-Moya A, Wiencke C (1998) An inventory of UV-absorbing mycosporine-like amino acids in macroalgae from polar to warm-temperate regions. Bot Mar 41:443–445
Landy J, Ehn J, Shields M, Barber D (2014) Surface and melt pond evolution on landfast first-year sea ice in the Canadian Arctic Archipelago. J Geophys Res Oceans 119:3054–3075, doi:10.1002/2013JC009617
Lund JWG, Kipling C, Le Cren ED (1958) The inverted microscope method of estimating algal number and the statistical basis of estimations by counting. Hydrobiologia 11:143−170
Manney GL, Santee ML, Rex M, Livesey NJ, Pitts MC, Veefkind P, Nash ER, Wohltmann I, Lehmann R, Froidevaux L, Poole LR, Schoeberl MR, Haffner DP, Davies J, Dorokhov V, Gernandt H, Johnson B, Kivi R, Kyro E, Larsen N, Levelt PF, Makshtas A, McElroy CT, Nakajima H, Concepcion Parrondo M, Tarasick DW, von der Gathen P, Walker KA, Zinoviev NS (2011) Unprecedented Arctic ozone loss in 2011. Nature 478:469–475
Marchant HJ, Davidson AT, Kelly GJ (1991) UV-B protecting compounds in the marine alga *Phaeocystis pouchetii* from Antarctica. Mar Biol 109:391–395
Maslanik J, Stroeve J, Fowler C, Emery W (2011) Distribution and trends in Arctic sea ice age through spring 2011. Geophys Res Lett 38:L13502, doi: 13510.11029/12011GL047735
Medlin LK, Hasle GR (1990) Some *Nitzschia* and related diatom species from fast ice samples in the Arctic and Antarctic. Polar Biol 10:451–479
Medlin LK, Priddle J (1990) Polar marine diatoms. British Antarctic Survey, Cambridge
Mundy CJ, Gosselin M, Ehn JK, Belzile C, Poulin M, Alou E, Roy S, Hop H, Lessard S, Papakyriakou TN, Barber DG, Stewart J (2011) Characteristics of two distinct high-light acclimated algal communities during advanced stages of sea ice melt. Polar Biol 34:1869–1886
Mundy CJ, Gosselin M, Gratton Y, Brown K, Galindo V, Campbell K, Levasseur M, Barber D, Papakyriakou T, Bélanger S (2014) Role of environmental factors on phytoplankton bloom initiation under landfast sea ice in Resolute Passage, Canada. Mar Ecol Prog Ser 497:39–49
Nicolaus M, Katlein C, Maslanik J, Hendricks S (2012) Changes in Arctic sea ice result in increasing light transmittance and absorption. Geophys Res Lett 39:L24501, doi:10.1029/2012GL053738
Oren A (1997) Mycosporine-like amino acids as osmotic solutes in a community of halophilic cyanobacteria. Geomicrobiol J 14:231–240
Parsons TR, Maita Y, Lalli CM (1984) A manual of chemical and biological methods for seawater analysis. Pergamon, Oxford, UK

Perovich DK (2006) The interaction of ultraviolet light with Arctic sea ice during SHEBA. Ann Glaciol 44:47–52
Piiparinen J, Enberg S, Rintala J-M, Sommaruga R, Majaneva M, Autio R, Vähätalo AV (2015) The contribution of mycosporine-like amino acids, chromophoric dissolved organic matter and particles to the UV protection of sea-ice organisms in the Baltic Sea. Photochem Photobiol Sci 14:1025–1038
Poulin M (1993) *Craspedopleura* (Bacillariophyta), a new diatom genus of arctic sea ice assemblages. Phycologia 32:223–233
Poulin M, Cardinal A (1982a) Sea ice diatoms from Manitounuk Sound, southeastern Hudson Bay (Quebec, Canada). I. Family Naviculaceae. Can J Bot 60:1263–1278
Poulin M, Cardinal A (1982b) Sea ice diatoms from Manitounuk Sound, southeastern Hudson Bay (Quebec, Canada). II. Family Naviculaceae, genus *Navicula*. Can J Bot 60:2825–2845
Poulin M, Cardinal A (1983) Sea ice diatoms from Manitounuk Sound, southeastern Hudson Bay (Quebec, Canada). III. Cymbellaceae, Entomoneidaceae, Gomphonemataceae, and Nitzschiaceae. Can J Bot 61:107–118
Tomas CR (1997) Identifying marine phytoplankton. Academic Press, San Diego
Rex M, Harris NRP, von der Gathen P, Lehmann R, Braathen GO, Reimer E, Beck A, Chipperfield MP, Alfier R, Allaart M, Oconnor F, Dier H, Dorokhov V, Fast H, Gil M, Kyro E, Litynska Z, Mikkelsen IS, Molyneux MG, Nakane H, Notholt J, Rummukainen M, Viatte P, Wenger J (1997) Prolonged stratospheric ozone loss in the 1995–96 Arctic winter. Nature 389:835–838
Ryan KG, McMinn A, Mitchell KA, Trenerry L (2002) Mycosporine-like amino acids in Antarctic sea ice algae, and their response to UVB radiation. Z Naturforsch 57c:471–477
Shick JM, Dunlap WC (2002) Mycosporine-like amino acids and related gadusols: Biosynthesis, accumulation, and UV-protective functions in aquatic organisms. Ann Rev Physiol 64:223–262
Sinha RP, Klisch M, Gröniger A, Häder DP (2001) Responses of aquatic algae and cyanobacteria to solar UV-B. Plant Ecol 154:221–236
Sommaruga R, Chen YW, Liu ZW (2009) Multiple strategies of bloom-forming *Microcystis* to minimize damage by solar ultraviolet radiation in surface waters. Microb Ecol 57:667–674
Spence E, Dunlap WC, Shick JM, Long PF (2012) Redundant pathways of sunscreen biosynthesis in a cyanobacterium. ChemBioChem 13:531–533
Suh HJ, Lee HW, Jung J (2003) Mycosporine glycine protects biological systems against photodynamic damage by quenching singlet oxygen with a high efficiency. Photochem Photobiol 78:109–113
Thomsen HA (1992) Plankton i de indre danske farvande. Havforskning fra Miljøstyrelsen, Volume 11. Scantryk, Copenhagen
Tomas CR (1997) Identifying marine phytoplankton. Academic Press, San Diego, CA
Uusikivi J, Vahatalo AV, Granskog MA, Sommaruga R (2010) Contribution of mycosporine-like amino acids and colored dissolved and particulate matter to sea ice optical properties and ultraviolet attenuation. Limnol Oceanogr 55:703–713
Villafañe VE, Barbieri ES, Helbling EW (2004) Annual patterns of ultraviolet radiation effects on temperate marine phytoplankton off Patagonia, Argentina. J Plankton Res 26:167–174

Volkmann M, Gorbushina AA, Kedar L, Oren A (2006) Structure of euhalothece–362, a novel red-shifted mycosporine-like amino acid, from a halophilic cyanobacterium (*Euhalothece* sp.). FEMS Microbiol Lett 258:50–54

von Quillfeldt CH (1997) Distribution of diatoms in the Northeast Water Polynya, Greenland. J Mar Syst 10:211–240

Whitehead K, Karentz D, Hedges JI (2001) Mycosporine-like amino acids (MAAs) in phytoplankton, a herbivorous pteropod (*Limacina helicina*), and its pteropod predator (*Clioneantarctica*) in McMurdo Bay, Antarctica. Mar Biol 139:1013–1019

Zhang Z, Tashiro Y, Matsukawa S, Ogawa H (2005) Influence of pH and temperature on the ultraviolet-absorbing properties of porphyra-334. Fisheries Sci 71:1382–138

Chapter 3: Method Development for the Isolation of an Unknown UV-Absorbing Compound Present in First-Year Sea Ice Melt Ponds

Abstract:

Following the observation of a unique UV-absorbing compound (U2) naturally occurring in sea ice melt pond particulate in the Arctic springtime, isolation of this compound was pursued for the purpose of structural elucidation. Two HPLC methods from the literature that are currently used for the separation of mycosporine-like amino acids as well as one that is used for the separation of polar compounds that contain a carboxylic acid functional group were examined. Unsuccessful isolation of U2 with these methods led to an attempt to strategically modify the method that was used to identify it in samples (Carreto et al. 2005). From these analyses, it was determined that the best method for isolation involves modification of the pH of the mobile phase in the Carreto method.

3.1 Introduction

Currently, the Arctic is undergoing rapid climatic changes that have resulted in a decrease in the aerial coverage and thickness of sea ice at its minimum extent (Comiso et al. 2008) as well as a later freeze-up and an earlier melt onset (Maslanik et al. 2011). These changes are predicted to increase ultraviolet (UV) radiation transmission through sea ice (Perovich 2006); this would ultimately increase exposure to ice-associated Arctic marine organisms. In addition to climatic changes, ozone reduction in the Arctic stratosphere has also been observed more frequently in recent years (Manney et al. 2011), which will also lead to increased exposure of Arctic organisms to UV radiation.

Most primary producers living beneath or within sea ice are adapted to acclimate to low light conditions (Thomas & Dieckmann 2009) due to the need to overcome long dark winters and light attenuation by the snow and ice cover. However, high-light acclimation has been shown to be an important strategy for ice-associated algae during the ice melt period (Mundy et al. 2011, Alou et al. 2013, Piiparinen et al. 2015). Little is known about the ability of algae in this region to acclimate to high UV-light.

The production of sun-screening compounds as secondary metabolites is one way in which organisms can acclimate quickly to high UV-exposure. The most prevalent group of sun-screening compounds in marine algae is mycosporine-like amino acids (MAAs) that are able to screen incoming UVA (280-400 nm) (Gao & Garcia-Pichel 2011). MAAs function by absorbing incoming high-energy radiation and dissipating the energy as heat into the surroundings (Conde et al. 2000). There has been a lot of discussion regarding the possibility of these metabolites playing multiple functions for an organism. Other roles such as an antioxidant (Dunlap & Yamamoto 1995) and osmotic protectants (Oren 1997) have also been investigated. Antioxidants are also beneficial under high UV-stress since reactive oxygen species are produced indirectly in photosynthesizers exposed to high-light conditions. Furthermore, MAAs have been demonstrated to be an effective photo-protectant by decreasing levels of photoinhibition caused by UV radiation in dinoflagellates who produce them (Neale et al. 1998). The use of MAAs is one of many ways in which organisms can sustain photosynthesis under high UV radiation conditions.

Following the analysis of samples collected throughout the spring melt transition in Allen Bay, NU we observed the presence of three MAAs, shinorine, porphyra-334 and palythine, as well as two unknown UV-absorbing compounds (UVACs) (Elliott et al. 2015; Chapter 2). In newly formed melt ponds an unknown UVAC (U2) was observed in almost all samples.

Shinorine (structure shown in Figure 1.3, Chapter 1) was the only known MAA detected in melt pond samples containing U2. U2 was also detected in bottom ice communities beneath melt ponds as well as under ice melt communities beneath melt ponds. Relatively high absorbance was measured for this compound and it had an absorption spectra with two absorption maxima, one at 363 nm and a shoulder peak at 337 nm (see Figure 3.2; Figure 2.4, Chapter 1). A similar UV-absorbing compound, which displayed comparable absorption and high performance liquid chromatography (HPLC) elution characteristics, was reported in Piiparinen et al. (2015) whose dataset came from ice-associated algae from the Baltic Sea. Furthermore, similar absorption characteristics to U2 have been observed in melt pond algae collected from first-year ice in the western Canadian Arctic (Mundy et al. 2009). There is interest in isolating and elucidating the structure of this unknown component in melt ponds in order to understand if there are unique UV-screening molecules in this habitat that may be important for primary producers associated with the sea ice cover during the sea ice melt transition.

In this chapter I describe my attempts to isolate U2 for structural identification. U2 was not retained on our reverse phase analytical column, therefore our first hypothesis was that it was a highly polar organic compound that favored the aqueous mobile phase. The MAA with the most similar separation in our analytical method was shinorine, a polar and acidic MAA. It contains two carboxylic acid functional groups that are responsible for its acidic properties (Figure 1.3, Chapter 1). My initial attempts at isolation were based on this hypothesis.

3.2. Materials and Methods

3.2.1 Sampling

Two sets of field samples were used for testing purposes in this study. Samples from surface melt ponds were collected from Allen Bay, Nunavut, Canada at an ice camp field site

(74°43’ N, 95°09’ W) as part of the Arctic-ICE (Ice Covered Ecosystem) program. Samples were collected following the development of melt ponds, June 12 in 2011 and June 13 in 2012. Details regarding environmental conditions such as temperature, ice thickness, water depth and light measurements for 2011 sampling period can be found in Elliott et al. (2015) (Chapter 2). Sampling of the surface melt ponds occurred every four days as part of a regular sampling schedule in 2011 and every two days in 2012. Slurp guns were used to collect surface melt pond samples in 2011 and were filtered onto glass fiber filters (GFF) with a nominal 0.7 μm mesh in an off-site laboratory (Elliott et al., 2015; Chapter 2). In 2012 large volume melt pond samples (~100 L) were collected with an iL280P portable pump (Xylem Inc., Westchester County, USA) into LDPE (low density polyethylene) collapsible plastic containers. They were then filtered onto 14.2 cm diameter GFF filters. Samples were stored at -20 °C until analysis. Samples were analyzed using the methods of Elliot et al. (2015; Chapter 2) to determine the presence of U2 prior to proceeding with further analyses described below.

3.2.2 Sample Analysis

MAA extraction followed the procedures described in Carreto et al. (2005; hereinafter the Carreto method) and Elliott et al. (2015) (Chapter 2). Following evaporation of methanol from the sample extracts the solvent used to reconstitute varied according to the starting mobile phase used for separation and detection. The extracts were then evaporated to dryness under nitrogen at a temperature of 50°C and reconstituted with the mobile phase used in the HPLC method. The analysis was done on an Agilent 1200 HPLC coupled to an Agilent 6410B electrospray ionization triple quadrupole mass spectrometer (ESI-QQQ-MS) and an Agilent 1100 diode array and multiple wavelength detector (DAD). The HPLC method used in the initial observation of our Unknown (U2) was the Carreto method (Elliott et al., 2015; Chapter 2). Formic acid was

used instead of trifluoroacetic acid as was suggested by Carignan et al. (2009) for optimization of the method to electrospray ionization. The QQQ was set to scan between 100-1000 mass to charge ratio (m/z), with a nebulizer pressure of 60 psi, gas flow rate 11 L min^{-1} and source temperature set to 325°C for scanning purposes. To verify the presence of shinorine, palythine and porphyra-334 we used the multiple reactions monitoring method as described in Elliott et al. (2015) (Chapter 2). The DAD continually recorded the absorbance spectra between the wavelengths 190 and 600 nm. Absorbance was also monitored continually at the specific wavelengths 310, 320, 330, 360 and 250 nm. The instrument path length was 10 mm and the slit width was set to 4 nm, response time to 2.0 s and step to 2 nm. The DAD parameters were kept constant for all methods used in this study.

For the particular comparison of absorption properties of our unknown in different mobile phases (methods 1a-e) a single high volume field sample (96 L) was extracted with 20 mL of methanol twice (for a total of 40 mL). Subsamples were taken of equal volume 6 mL in order to obtain identical samples for comparison. Hereinafter, these subsamples are referred to as "U2-test standards". The Carreto method (method 1, Table 3.1) was then adjusted systematically to observe changes in the separation of U2. Methanol content was adjusted first and an isocratic elution over 50 min was observed. The mobile phases investigated were 0% methanol (method 1a, Table 3.1), 5% methanol (method 1b, Table 3.1), 10% methanol (method 1c, Table 3.1) and 50% methanol (method 1d, Table 3.1). For all the methods 1a-d 0.2% formic acid was present and the pH of the mobile phase was adjusted to 3.15 with ammonia hydroxide. Second, we observed the effect of adjusting the pH from 3.15 to a pH or 5.8 with a mobile phase with a methanol content of 0% (method 1e, Table 3.1). Again an isocratic elution over 50 minutes was observed.

Table 3.1 HPLC methods adapted to attempt the separation of U2 from known mycosporine-like amino acids (MAAs). "MAAs separated" identifies the elution order of MAAs separated in the original paper. The number in brackets refers to the retention time either estimated from published chromatograms or given directly in the literature (Stochaj et al. 1994),(Carreto et al. 2005),(Sleeman et al. 2005). (TFA = trifluoroacetic acid).

Method I.D.	Methods Paper	Stationary Phase	Mobile Phase	MAAs Separated	Detector
1	Carreto et al. 2005	Polymeric double end-capped C18 (150 mm × 4.6 mm i.d., 5 μm) and a polymer coated silica reverse-phase C18 column (250 mm × 4,6 i.d., 5 μm)	A: Water with 0.2% TFA adjusted to a pH = 3.15 with ammonium hydroxide B: 80:10:10 water:methanol: acetonitrile with 0.2% TFA adjusted to a pH = 2.2 with ammonium hydroxide	Palythine-serine sulfate (4.76), mycosporine sulfate ester (5.25), shinorine (5.65), mycosporine-2-glycine (6.19), palythine-serine (6.68), palythine (7.52), asterine (8.43), porphyra-334 (8,87), mycosporine-methylamine-serine (9.60), mycosporine-glycine (10.11), palythinol (13.26), Z-palythenic acid (13.83), shinorine methyl ester (14.10), E-palythenic acid (15.97), M-320 (19.54), usujirene (28.95), palythene (29.94), M-335/360 (35.71)	Absorbance at 360, 330, 310 and 270 nm and absorbance spectra using a diode array detector
1a	n/a	Same column as method 1	Water with 0.2% TFA adjusted to a pH = 3.15 with ammonium hydroxide	n/a	Absorbance at 360, 330, 320, 310 and 250 nm and ESI mass spectrometer
1b	n/a	Same column as method 1	Water with 5% Methanol 0.2% TFA adjusted to a pH = 3.15 with ammonium hydroxide	n/a	Same as method 1a
1c	n/a	Same column as method 1	Water with 10% Methanol 0.2% TFA adjusted to a pH = 3.15 with ammonium hydroxide	n/a	Same as method 1a
1d	n/a	Same column as method 1	Water with 50% Methanol 0.2% TFA adjusted to a pH = 3.15 with ammonium hydroxide	n/a	Same as method 1a

1e	n/a	Same column as method 1	Water with 0.2% TFA adjusted to a pH = 5.79 with ammonium hydroxide	n/a	Same as method 1a
2	n/a	Shiseido capcall core ADME column (100 mm X 2.1 mm i.d., 2.7 µm)	Same as method 1a	n/a	Same as method 1a
3	Stochaj et al. 1994	Brownlee Speri-5 RP-8 column with RP-8 guard column	75% Methanol 0.1% Acetic acid	mycosporine-taurine (4.5), shinorine (15), porphyra-334 (17), mycospoine-2-glycine (19)	Absorbance at 340 nm
4	Sleeman et al. 2005	µBondpak NH2 (270 mm X 4.6 mm i.d.)	A: 5% methanol B: 5% MeOH with 0.05% formic acid	none	Micro-mass ZMD mass spectrometer

Three other reverse phase HPLC methods were attempted in order to obtain a good separation of U2. Method 2 (Table 3.1) followed the same conditions used in method 1, but employed a Shiseido capcall core adamantyl function group (ADME) column (100 mm, 2.7 µm particle size, 2.1 mm i.d.) to attempt to increase the retention of more polar compounds on the column.

Method 3 followed the method of Stochaj et al. (1994; Table 3.1), which was adapted from the original method by Dunlap and Chalker (1986). It involved an isocratic elution with a mobile phase containing 75% methanol with 0.2% acetic acid at 0.8 mL min^{-1}. The column used was a Spheri-5 RP-8 (250 mm, 5 µm particle size, 4.6 mm i.d.) (PerkinElmer) with an analytical C8 guard column (PerkinElmer).

The final method (method 4; Table 3.1) attempted was adapted from Sleeman et al. (2005). A µBondpak NH2 (270 mm X 4.6 mm i.d.) column (Waters) equilibrated in 5% MeOH at 1.5 mL min^{-1} was used. A gradient elution program was used that started with the 5%

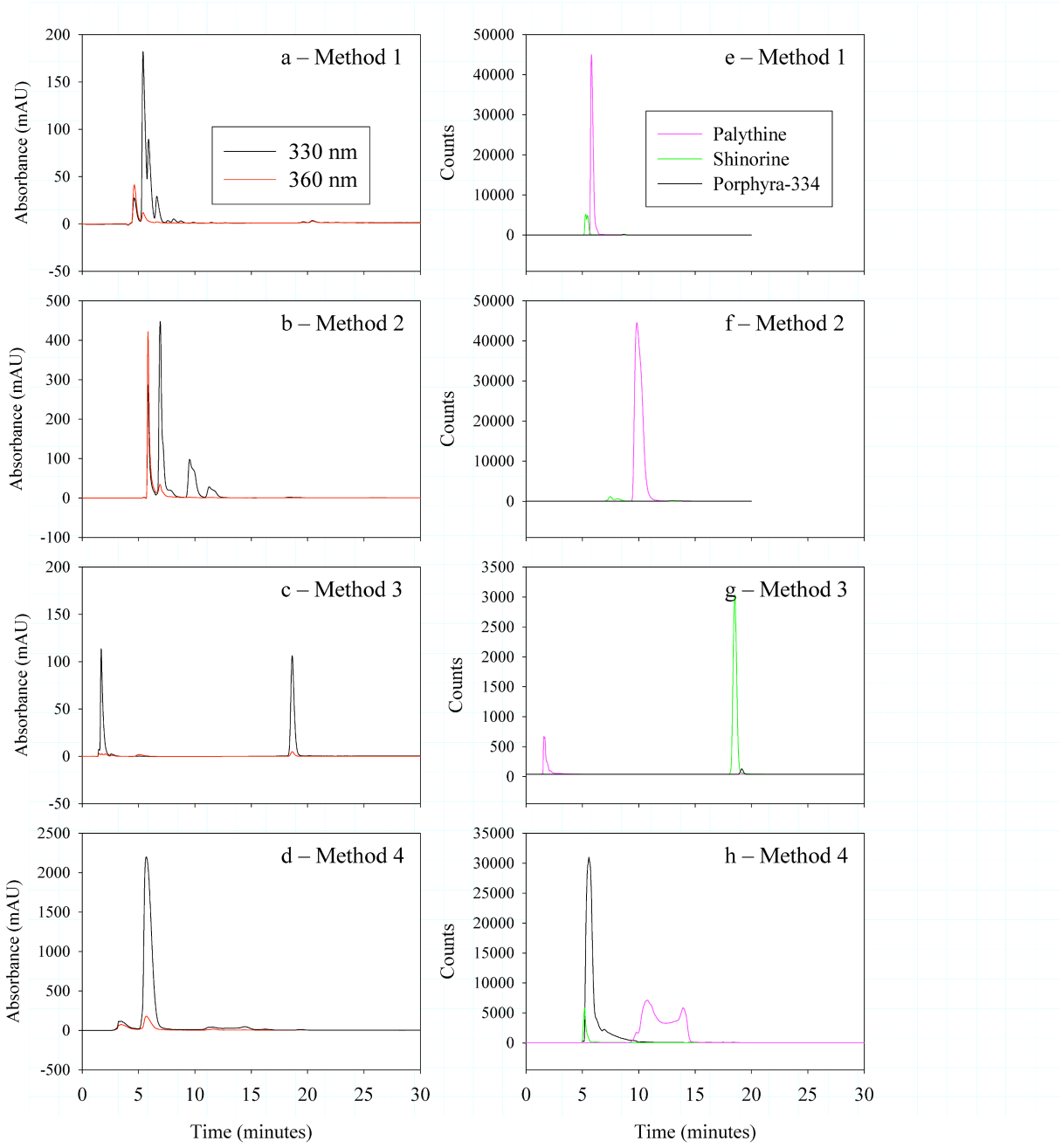

Figure 3.1 Chromatograms obtained from field samples (a-c and e-g) and seaweed samples (d and h) using several different methods. Chromatograms a-e were collected using absorbance detector and chromatograms f-h were collected using multiple reaction monitoring method with a triple quadrupole mass spectrometer. a and e) Melt pond samples collected June 15 2012 analyzed using method 1 with modification, b and f) Melt pond sample collected June 17 2012 analyzed using method 2, c and g) "" analyzed using method 4 and d and h) seaweed sample (Porphyra sp.) analyzed using method 3.

methanol at 100% for 5 minutes. After 5 min, a gradient to 5% MeOH with 0.05% formic acid

was run over 10 min. Changes were made after initial attempts, we equilibrated the column with 5% methanol and then ran the samples with 5% methanol and 0.2% formic acid over 20 min. The column was re-equilibrated for 20 min between samples with 5% methanol. An isocratic elution with 100% methanol over 40 min was also performed.

3.3 Results

3.3.1 Methods 1-4

Method 1 (Carreto method) was the same method used in Elliott et al (2015) (Chapter 2) and has remained our most reliable method for the identification of U2 in a field sample (Figure 3.1a, e). Under the Carreto method U2 is eluted at 4.6 min with a characteristic dual absorption maxima spectrum showing a peak at 363 nm and shoulder peak at 337 nm (Figure 3.2). This method was used to screen field samples to determine if they contain U2. The separation of U2 from other MAAs in our sample was sufficient as the baseline was separated from the closest eluting MAA shinorine. However, the separation from other (non-UV-absorbing) compounds was insufficient, as the baseline was not well separated from the breakout peak. The breakout peak was defined as the first peak eluted from the column and typically contained a mixture all the components of the sample that were retained during extraction and clean-up of the samples, but were not retained on the column. There was no separation of these components because they do not interact with the stationary phase of the column. The breakout peak was typically identifiable by a change in the baseline. In our field blank samples (filtered sea water) the breakout peak was thought to contain primarily salts (Elliott et al. 2015; Chapter 2).

Method 2 (Figure 3.1b and 3.1f) did not provide any greater retention of U2. The apparent greater retention time (~5.1 minutes, Figure 3.1b) was due to the slower flow rate used in the method. Again, a baseline separation was not obtained from the breakout peak. Field

samples that were run were previously screened and known to contain U2 as well as at least one other known MAA. Better separation was observed of known MAAs (shinorine and palythine)

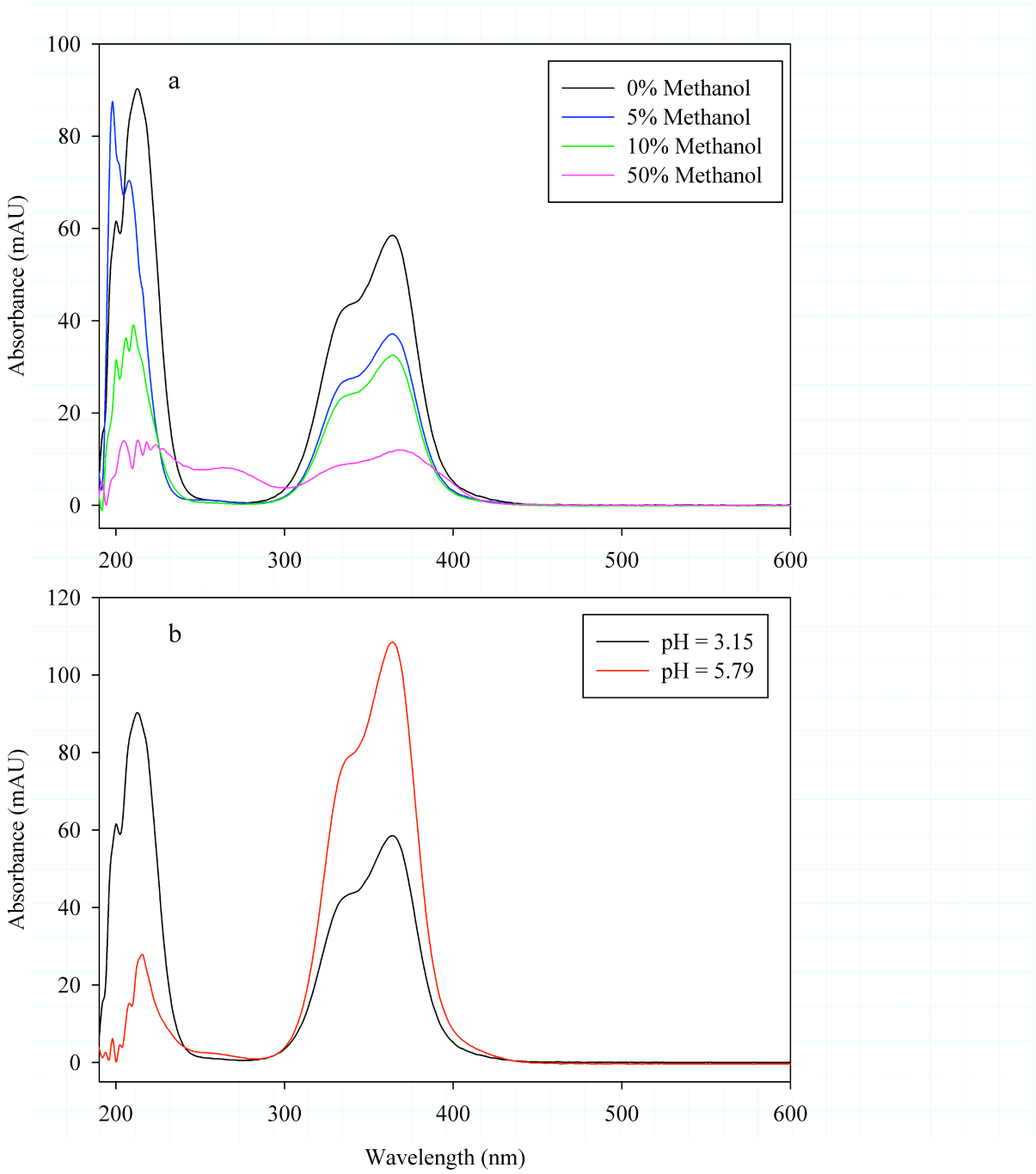

*Figure 3.2 Absorbance spectra of unknown compound in field samples (melt pond sample collected June 17 2012 from first year fast ice) collected using a diode array detector. a) Method 1a and 1e was used with a modification to an isocratic elution with a mobile phase containing 0% methanol and modified pH, **b**) Method 1a-d used. The pH of all mobile phases and samples was adjusted to 3.15.*

but the peak shape was poorer with a non-Gaussian distribution.

Method 3 was run initially with a field sample known to contain U2 and failed to separate U2 in the observed peaks. Method 3 was also run with a seaweed sample (Porphyra *spp.*) that contained shinorine, palythine and porphyra-334 and the results were not consistent with what was reported in the literature (Figure 3.1d, h). Greater retention of the more acidic MAAs, as shown in the Stochaj et al. (1994) work, was not obtained. Very broad and undefined peak shapes in all of our analyses were also observed and the resulting retention times for known MAAs were inconsistent.

Method 4 (with 0.05% formic acid in mobile phase 2) yielded inconsistent retention times for the more acidic MAAs such as shinorine and porphyra-334. Upon increasing the volume of acid added to the mobile phase to 0.2% by volume and starting the method with mobile phase B at the beginning of the analytical method, more consistent results were obtained (Figure 3.1c, g). The column did not retain Palythine, while porphyra-334 and shinorine were retained and eluted at approximately 18.5 minutes. U2 was not identified within the resulting chromatograms when running the field samples known to contain the unknown.

3.3.2 Modifications to Method 1

The addition of methanol to the mobile phase did not provide any increased separation of U2 from the breakout peak. As the percentage of methanol was increased, the retention of shinorine and palythine decreased, which resulted in overlap of known MAAs and U2. At 50% methanol by volume the known MAAs were eluted just prior to U2 with near baseline separation (Figure 3.3).

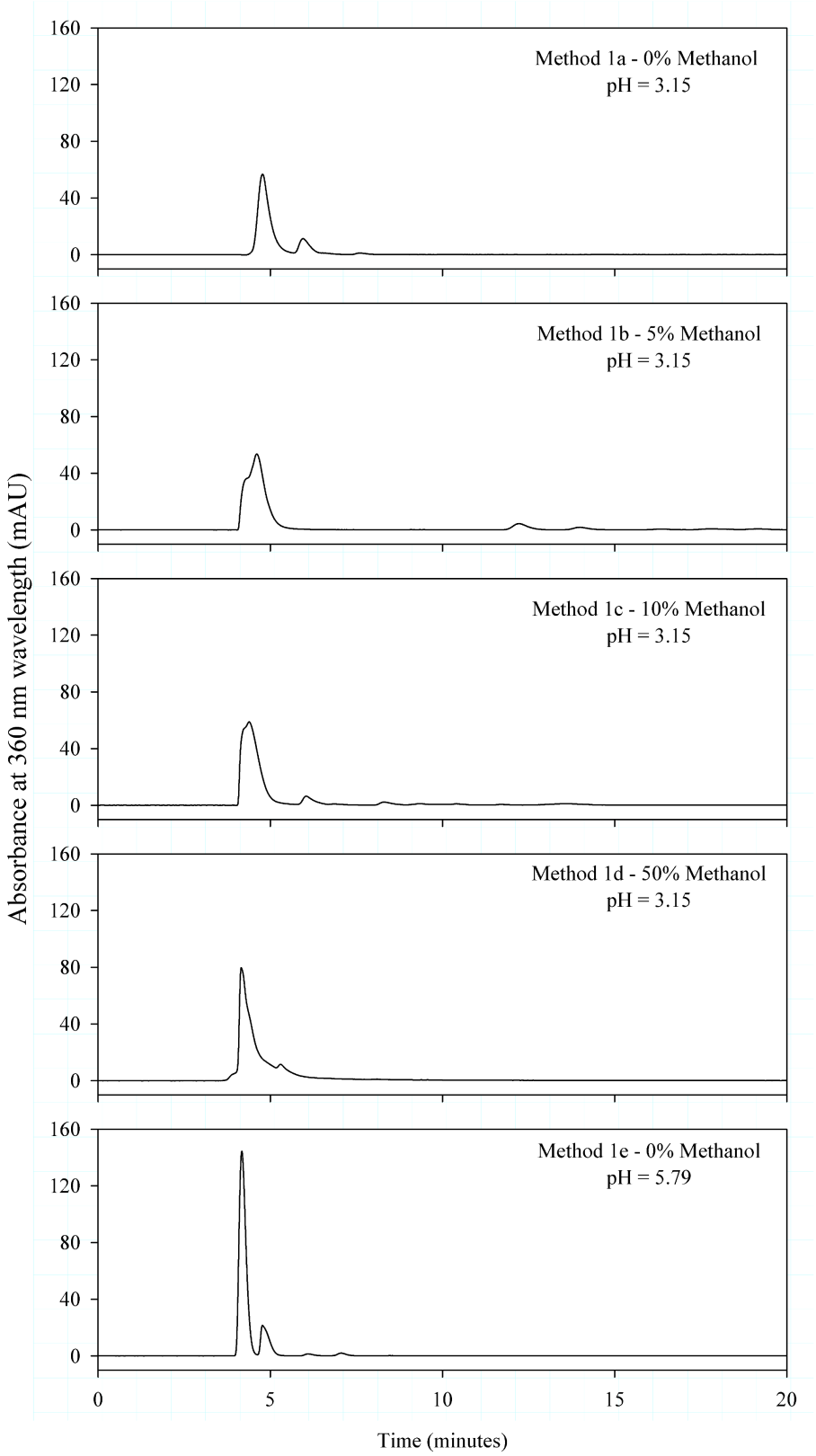

Figure 3.3 Separation of U2 using modifications to method 1. Absorption spectra in Figure 3.2 were taken from the same analytical run at 4.8, 4.4, 4.2, 5.4 and 4.2 minutes for methods 1a-e respectively.

The pH of the mobile phase was also modified to determine if we could obtain greater separation of U2. The best baseline separation of U2, from both the known MAAs and the breakout peak, was observed at a pH of 5.8. This separation was accompanied by peak broadening, but the peaks maintained a Gaussian distribution (Figure 3.3).

3.4 Discussion

3.4.1 Method Reproducibility

Unfortunately, method 4 could not be successfully reproduced. This method has been mentioned in the review of Carreto and Carignan (2011) as a unique method due to its ability to separate more polar and acidic MAAs. The rationale for increased separation was based on increased interaction of these MAAs with the stationary phase. The increased interaction with the stationary phase in this method was due to the high proportion of methanol in the mobile phase and interaction of acidic MAAs with non-endcapped silanol groups on the stationary phase since the stationary phase contained non-endcapped silanol groups. The method has not been popular in other works likely because it is unable to separate less polar and weakly acidic MAAs and thus more than one method would be required to identify MAAs in a sample. The conditions described in the original paper were replicated to our best ability, but a high retention of shinorine or porphyra-334 was not observed. Peak shape was also broader and less defined as shown in the original work and retention times for porphyra-334 and shinorine were not consistent (Stochaj et al. 1994).

3.4.2 Spectral Properties of Unknown

During attempts to isolate U2, the composition of the mobile phase seemed to affect the spectral properties of the unknown. As the percentage of methanol by volume was increased in

the mobile phase using method 1, a decrease in the absorption at 363 and 337 nm was observed (Figure 3.2a) while the ratio of the two peaks remained the same. An increase in the absorption at 363 and 337 nm was also observed when the pH was increased (Figure 3.2b). It is impossible to quantify this observation at this time due to a lack of a purified sample to analyze. The samples used are identical but the peak shape and separation from other sample components is adjusted as the method conditions are adjusted. The decreasing trend in U2 absorption characteristics with increases in methanol concentration likely explains why U2 was not identified using method 3 where the methanol conent in the mobile phase is 75%.

3.4.3 Identity of U2

Upon observing the characteristic spectra with two absorption peaks it was surmised that the observed spectra could be due to two compounds that eluted from the column simultaneously (Elliott et al., 2015; Chapter 2). In any modified method where a shift in the retention of the unknown was detected, the absorption spectra were intact. Furthermore, decreases in absorption with changing mobile phase did not result in a shift in only one of the absorption maxima but in both simultaneously. Therefore, U2 is likely a single compound with two absorption maxima as opposed to a mixture of two different compounds.

The methods used in this chapter were chosen primarily based on the hypothesis that U2 is a MAA similar to the most polar MAA (shinorine). The results suggest that this hypothesis is likely false since the compound does not seem to have similar chemical properties as shinorine. For example, shinorine was retained on an amino column using Method 4. The amino column should retain compounds that contain a carboxylic acid group at a neutral pH and as the pH of the column is decreased using a mobile phase containing formic acid the compounds are eluted based on their differences in their acid dissociation constants. Shinorine and porphyra-334 were

both retained through this process but U2 was not observed. It follow that U2 likely does not have a similar structure to shinorine and porphyra-334.

The spectral properties of U2 seem to be greatly affected by the matrix in which it is contained. Although the data presented was not conclusive since the observations are not quantified, the observed trend is interesting and indicates that the capacity of the compound to absorb radiation was affected by both pH and methanol concentration. The trend may help explain why the unknown was not identified in certain analytical conditions such as with method 4 that had a methanol content of 75%. The matrix effects on the extinction coefficient of MAAs are not well studied with the exception of porphyra-334 (Zhang et al. 2005). Porphyra-334 did not show the same changes in spectral properties that were observed with U2. These results suggest that U2 may be unrelated structurally to MAAs and its absorbing capacity may be strongly affected by pH because of acidic or basic functional groups. The strong change in absorption properties with changing pH may indicate that the deprotonated form of the molecule absorbs light with peaks at the observed maxima and the protonated form does not.

3.4.4 Future work

The main barrier to identification of U2 is producing a sample with enough mass and purity for the chemical analysis. Therefore the focus of future research should be to collect U2 using HPLC Method 1d for structural identification. One barrier to this is obtaining field samples containing U2, which can be cost and time intensive. The appearance of U2 in samples in the same region over two sampling seasons is encouraging. Furthermore, the unknown identified as M335/360 in Baltic sea ice (Piiparinen et al. 2015) appeared to have strong similarities to U2 therefore, could support a ubiquitous presence of U2 in melting Arctic sea ice. The best analytical technique is likely nuclear magnetic resonance (NMR) for several reasons. Firstly, it is

non-destructive and will allow the analyst to run several methods without consuming the limited sample available. Secondly, NMR spectra are available for many MAAs such as mycosporine-glycine, palythine, palythinol, palythene (takano et al 1978), providing a library of MAA spectra to compare with the U2 spectra. Lastly, NMR will give convincing evidence on whether U2 is of organic or inorganic nature. Chemical assays such as acid hydrolysis and amino acid assays can also be done if NMR results provide some idea of the nature of U2. Other analytical techniques that can be employed are tandem mass spectrometry following direct injection into the electrospray ionization chamber. This will provide crucial information on the mass of U2, but the main drawback is the difficulty in getting a good signal in an aqueous mobile phase. Ideally the aqueous sample would be evaporated to dryness and reconstituted with methanol or acetonitrile.

Literature Cited

Alou E, Mundy CJ, Roy S, Gosselin M, Agusti S (2013) Snow cover affects ice algae pigment composition in the coastal Arctic Ocean during the spring-summer transition. Mar Ecol-Prog Ser 474:89-104

Carreto JI, Carignan MO (2011) Mycosporine-Like Amino Acids: Relevant Secondary Metabolites. Chemical and Ecological Aspects. Mar Drugs 9:387-446

Carreto JI, Carignan MO, Montoya NG (2005) A high-resolution reverse-phase liquid chromatography method for the analysis of mycosporine-like amino acids (MAAs) in marine organisms. Mar Biol 146:237-252

Comiso JC, Parkinson CL, Gersten R, Stock L (2008) Accelerated decline in the Arctic sea ice cover. Geophys Res Lett 35

Conde FR, Churio MS, Previtali CM (2000) The photoprotector mechanism of mycosporine-like amino acids. Excited-state properties and photostability of porphyra-334 in aqueous solution. J Photochem Photobiol B-Biol 56:139-144

Dunlap WC, Chalker BE (1986) Identification and quantitation of near-UV absorbing compounds (S-320) in a hermatypic scleractinian Coral Reefs 5:155-159

Dunlap WC, Yamamoto Y (1995) Small-molecule antioxidants in marine organisms: Antioxidant activity of mycosporine-glycine. Comp Biochem Phys B 112:105-114

Gao Q, Garcia-Pichel F (2011) Microbial ultraviolet sunscreens. Nat Rev Micro 9:791-802

Manney GL, Santee ML, Rex M, Livesey NJ, Pitts MC, Veefkind P, Nash ER, Wohltmann I, Lehmann R, Froidevaux L, Poole LR, Schoeberl MR, Haffner DP, Davies J, Dorokhov V, Gernandt H, Johnson B, Kivi R, Kyro E, Larsen N, Levelt PF, Makshtas A, McElroy CT, Nakajima H, Parrondo MC, Tarasick DW, von der Gathen P, Walker KA, Zinoviev NS (2011) Unprecedented Arctic ozone loss in 2011. Nature 478:469-U465

Maslanik J, Stroeve J, Fowler C, Emery W (2011) Distribution and trends in Arctic sea ice age through spring 2011. Geophys Res Lett 38

Mundy CJ, Gosselin M, Ehn JK, Belzile C, Poulin M, Alou E, Roy S, Hop H, Lessard S, Papakyriakou TN, Barber DG, Stewart J (2011) Characteristics of two distinct high-light acclimated algal communities during advanced stages of sea ice melt. Polar Biol 34:1869-1886

Neale PJ, Banaszak AT, Jarriel CR (1998) Ultraviolet sunscreens in Gymnoinium sanguineum (dinophyceae): mycosporine-like amino acids protect against inhibition of photosynthesis. J Phycol 34:928-938

Oren A (1997) Mycosporine-like amino acids as osmotic solutes in a community of halophilic cyanobacteria. Geomicrobio J 14:231-240

Perovich DK (2006) The interaction of ultraviolet light with Arctic sea ice during SHEBA. Annals of Glaciology 44:47-52

Piiparinen J, Enberg S, Rintala J-M, Sommaruga R, Majaneva M, Autio R, Vahatalo AV (2015) The contribution of mycosporine-like amino acids, chromophoric dissolved organic matter and particles to the UV protection of sea-ice organisms in the Baltic Sea. Photochem Photobiol Sci 14:1025-1038

Sleeman MC, Sorensen JL, Batchelar ET, McDonough MA, Schofield CJ (2005) Structural and mechnistic studies on carboxymethylproline synthase (CarB) a unique member of the

crotonase superfamily catalyzing the first step in carbapenem biosynthesis. J Biol Chem 280:34956-34965
Stochaj WR, Dunlap WC, Shick JM (1994) Two new UV-absorbing mycosporine-like amino acids from the sea anemone Anthropleura elegantissima and the effects on chemical composition and content. Mar Biol 118:149-156
Thomas DN, Dieckmann GS (2009) Sea Ice. Wiley
Zhang Z, Tashiro Y, Matsukawa S, Ogawa H (2005) Influence of pH and temperature on the ultraviolet-absorbing properties of porphyra-334. Fisheries Science 71:1382-1384

Chapter 4: Concluding Remarks

4.1 Summary of Findings

As stated in Chapter 1, my thesis objective was to identify which MAAs were present in the sea ice environment in the Canadian Arctic as well as to try and understand their temporal and spatial evolution. In such isolated regions much time and energy is spent obtaining samples over a considerable period of time in order to study processes. In this work we have achieved important insights into the spatial and temporal evolution of MAAs in sea ice-associated communities in relation to chlorophyll *a* production, temperature, salinity and taxonomic abundances. We have observed that the timing of MAA production occurs mainly during the sea ice melt transition. Detection of MAAs was negligible in the months of March-May in sea ice algae sampled, and increased to measurable concentrations in June, corresponding to the changing temperature and light conditions. Areas of the sea ice that we observed the greatest MAA/chl *a* ratios were in sea ice habitats that were experiencing rapid change and decreases in the chl *a* content per volume. The observations are consistent with the generally held view that photosynthetic organisms produce MAAs when experiencing stress due to UVR exposure in their environment. Furthermore, we see the production of these compounds at the greatest rates in habitats that are exhibiting decreases in Chl *a.* This may either be due to a loss in biomass overall in the community or due to a loss in Chl *a* per cell. Both processes indicate algal communities that are under high stress in their environment, which is likely due to changing light conditions. We identified three MAAs, shinorine, palythine and porphyra-334, in both the underlying water column and in the sea ice. Three unknown UV-absorbing compounds (U1, U2, and U3), with U1 being tentatively identified as palythene, were also detected in samples collected throughout the study. Of particular interest is that U2 was the most dominant UV-

absorbing compound in the surface melt pond particulate samples we collected. It had an absorption spectra unique relative to any known MAA. The continuation of this thesis work was then focused on trying to identify the unknown compound.

Considerable work has been spent attempting to isolate U2. Although we have been unsuccessful in our ultimate goal of identification, a foundation has been established for future work. We have eliminated many logical pathways for isolation, and provided the best pathways forward for success. Initially it was hypothesized that U2 was a very polar MAA similar to that of shinorine. Shinorine was also detected in many of the samples analyzed that contained U2. However, the analysis provided in Chapter 3 did not support this hypothesis. Through working with U2 under many analytical conditions we observed its behavior in different media and its unique spectral properties that provided hints as to its chemical nature. For example, its spectral properties were greatly affected by pH and the chemical composition of the mobile phase. This finding is inconsistent with what has been observed for MAAs and contributes to evidence indicating that it is likely not structurally related to this group of compounds. Research on MAAs and other UV-absorbing compounds in the Arctic is so limited that our contributions can have a big impact. Likely the greatest contribution of this work is our ability to now ask more informed questions going forward in this research area.

4.2 Future Work

The future work in this area of research should focus on three main objectives.

1) Identification of unknown UV-absorbing compounds present in melt pond communities during sea ice melt transition
2) Determination of the species that contribute the most to MAA production
3) Synthesis of MAA standards

The identity of U2 will provide much clarity to our results. If it is a biomolecule, but is dissimilar to MAAs, it would be fascinating to unveil its properties in comparison to known UV-screening compounds. It would also be important to determine how isolated or widespread it occurs, and whether it is unique to sea ice habitats. It is indeed exciting when the possibilities are numerous, but if nothing else the identity of U2 would clarify whether this compound is important for the surface melt pond communities for UV-protection, which has great bearing on this work.

Greater insight into the species responsible for MAA production in this habitat will provide greater precision in predictions of shifts in species composition that may be observed with changing light conditions in this region. There are few incidences of pennate diatoms that are known to produce MAAs, a dominant and important ice algal type. Evidence suggested that the production of MAAs in our samples was from flagellate species, but results were not conclusive and thus, determination of the important MAA producers in sea ice is an important area for further research. Much work must be done in order to provide any conclusive evidence on this matter. A possible route to attempt to identify algae species capable of producing MAAs would be to collect and culture suspect species in a laboratory setting. Suspect species are species that are suspected to produce MAAs from previous work, such as those that have shown a positive relationship with MAA abundance in chapter 2.

Working with MAAs has been difficult due to the inability to obtain a source for reliable and readily available standards. Testing of analytical procedures using a greater variety of purified compounds would strengthen the reliability of results. The availability of internal standards would enhance analytical techniques by determining the existence of matrix effects from field samples experienced when using different ionization techniques in mass spectrometry.

Mass spectrometry is being used more widely now to increase our ability to quantify MAAs reliably but a lot of work needs to be done before we approach results without some caution.

I am eager to see the development of this field of work and what revelations will be observed next. Discovering the Arctic ecosystem during a time when things are changing so rapidly is an incredible opportunity as a young scientist and has nurtured my natural scientific curiosity.